Building and Environment 266 (2024) 112037

Contents lists available at ScienceDirect

Building and Environment

journal homepage: www.elsevier.com/locate/buildenv

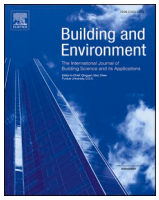

# Ventilation efficiency and improvements for displacement ventilation systems during heating: A case study of a ward with vertical induction units

Shaoyu Sheng [a,*], Toshio Yamanaka [b], Tomohiro Kobayashi [a], Nobukazu Chou [c]

[a] Department of Architectural Engineering, Graduate School of Engineering, Osaka University, 2-1 Yamadaoka, Suita, Osaka, 565-0871, Japan
[b] Institute for Open and Transdisciplinary Research Initiatives, Osaka University, 1-1 Yamadaoka, Suita, Osaka, 565-0871, Japan
[c] KIMURA KOHKI Co., Ltd, 5-3-5 Uehonmachinishi, Chuoku, Osaka, 542-0662, Japan

ARTICLE INFO

*Keywords:*
Displacement ventilation
Heating
Hospital ward ventilation
Induction unit
Full-scale experiment
CFD simulation

ABSTRACT

This study investigates the ventilation mechanism and effectiveness of a displacement ventilation (DV) system under heating conditions. A method to maintain ventilation efficiency by indirectly achieving DV was proposed. A four-bed hospital ward with prototype wall-mounted induction units (IUs) and ceiling exhaust served as the case study. Full-scale experiments assessed indoor temperature and tracer gas distribution, adjusting parameters such as cubicle and window curtains, window heaters, and window heat loss. Results showed that while the vertical temperature gradient was established, downdrafts near windows disrupted DV's stratification, leading to quasi-displacement ventilation with a normalized contaminant concentration of around 0.7 near patients. To counter this, using curtains to limit air exchange between the near-window and near-bed spaces effectively prevented the horizontal movement of contaminants toward the window. This allowed the downdraft to remain clean and diffuse along the floor, thereby reducing the normalized concentration to approximately 0.3–0.5 b y indirectly achieving DV. CFD numerical studies further examined this method under varied temperature conditions and airflow patterns. Additionally, the infection risk in this ward was evaluated for reference, showing that indirect DV can reduce infection probability by one-third compared to quasi-DV. Moreover, window heat loss valued at 50–100 W/m2 achieved the best ventilation, while smaller values generated insufficient downdraft to achieve indirect DV and larger values resulted in high floor-level velocity that accelerated contaminant dispersion.

Nomenclature

| | | | |
|---|---|---|---|
| C | Concentration (ppm) | **Abbreviations** | |
| $C_n$ | Normalized concentration | ACB | Active Chilled Beam |
| $I$ | Turbulence intensity (%) | ADPI | Air Diffusion Performance Index |
| $k$ | Kinetic energy ($m^2/s^2$) | CFD | Computational Fluid Dynamics |
| $l$ | Length of the roll curtain (m) | DV | Displacement Ventilation |
| $n$ | Quanta inhaled | EA | Exhaust Air |
| $q$ | Probability of infection | IA | Induction Air |
| $Q$ | Air flow rate ($m^3/h$) | IU | Induction Unit |
| $R_{mix}$ | Mixing ratio of the all-air induction unit | OA | Outdoor Air |
| $T$ | Airflow temperature (°C) | OCC | Outdoor Climate Chamber |
| **Greek Symbols** | | PA | Primary Air |
| $\varepsilon$ | Turbulence eddy dissipation ($m^2/s^3$) | SA | Supply Air |
| | | SKE | Standard $k$-$\varepsilon$ turbulence model |
| $\theta$ | Temperature (°C) | | |
| $\Delta\theta$ | Air temperature difference between the OCC's interior and the average air temperature at Fl+1.1m | | |
| **Subscripts** | | | |
| b | Breath | | |
| $n$ | Normalized | | |
| $P$ | Data sampling point | | |

(continued on next column)

(*continued*)

## 1. Introduction

Displacement ventilation (DV) is known for its high ventilation efficiency and lower energy consumption compared to conventional mixing ventilation [1–3]. In a typical DV system, conditioned fresh air is

* Corresponding author.
*E-mail address:* sheng_shaoyu@arch.eng.osaka-u.ac.jp (S. Sheng).

https://doi.org/10.1016/j.buildenv.2024.112037
Received 23 June 2024; Received in revised form 13 August 2024; Accepted 30 August 2024
Available online 31 August 2024

supplied from the lower part of the room. This airflow spreads across the floor, absorbing heat from sources such as occupants and electronic devices. The heated air then forms thermal plumes that rise to the ceiling due to buoyancy. Low-density pollutants, such as gaseous particles or certain virions, are transported upward in these thermal plumes to the ceiling space, where they are removed by exhaust vents installed in the ceiling. Studies and applications of DV systems have primarily focused on factories [4,5], office buildings [6,7], classrooms or lecture halls [8,9], large indoor spaces such as transportation terminals [10,11] and stadium [12,13], as well as the narrow spaces such as airliner [14] and

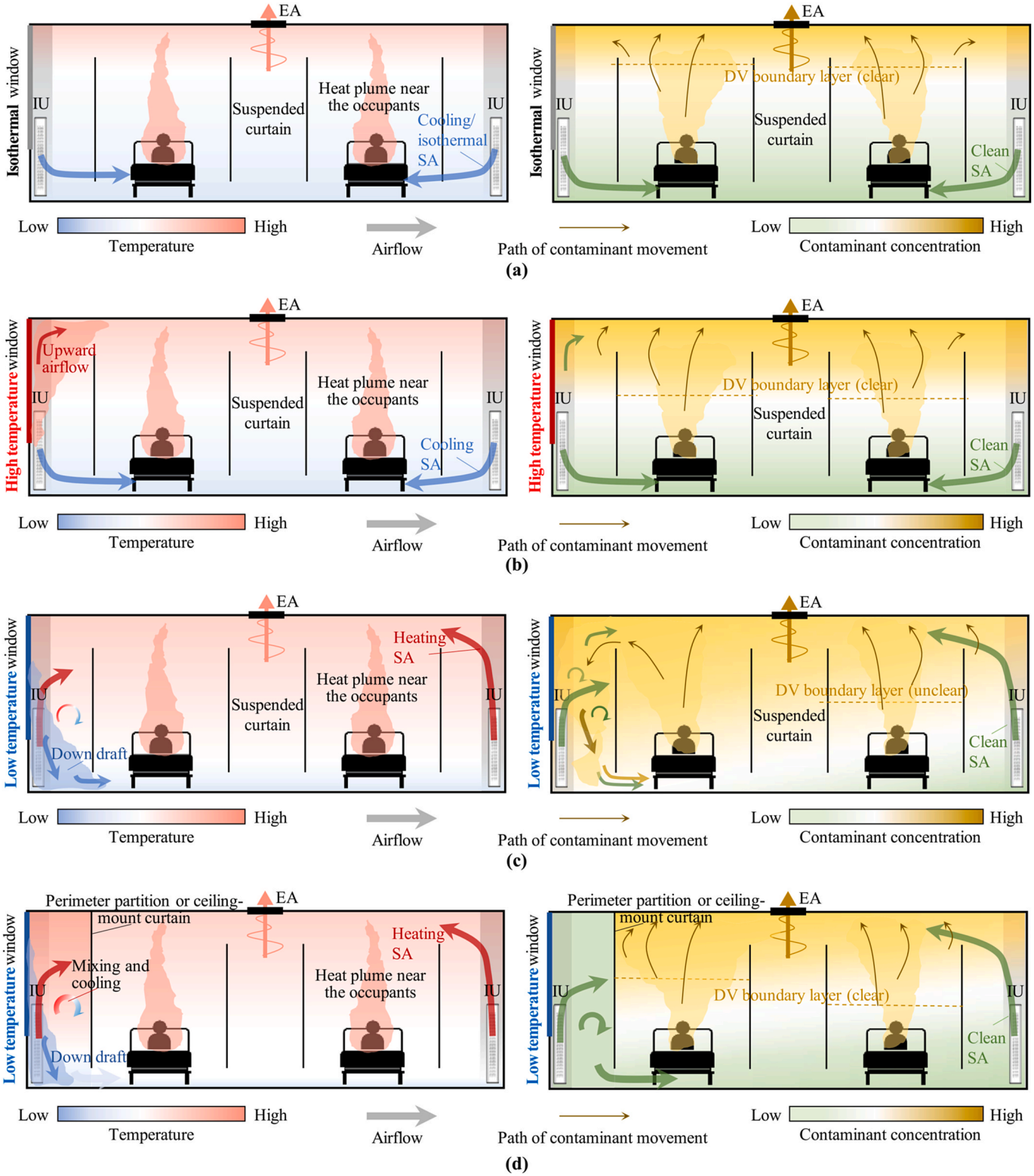


**Fig. 1.** Airflow pattern and air condition performance in a displacement ventilation room during different seasons. Improving winter ventilation by limiting horizontal contaminants movement and indirectly achieving DV through the downdraft. (a)shoulder season; (b) summer-cooling; (c) winter-heating; (d) improved the winter-heating.

train [15] cabins. Apart from its ventilation and energy efficiency, potential risks of DV, such as the impact of ceiling heights on the boundary layer, the influence of pollution source locations, the effects of flow elements and heat load, and thermal discomfort, have also been sufficiently investigated and identified as solvable issues in the aforementioned studies.

However, the DV system has a significant limitation: its effectiveness is mainly restricted to cooling or isothermal air supply and can be disrupted by the downward or upward airflow near walls or windows. Fig. 1 shows the temperature, airflow, and contaminant distribution in the room with the DV system during different seasons, illustrating varying ventilation efficiency. The background color indicates the temperature and contaminant concentration distribution. The thick arrows represent the supplied airflow or near-window airflow with different temperatures or concentrations. The thin arrows depict the route of contaminant movement.

During the shoulder season (Fig. 1(a)), similar indoor and outdoor temperatures allow the window to be considered an isothermal surface without affecting indoor airflow distribution. Cooling or isothermal SA is supplied into the occupied zone to handle indoor heat load or just for ventilation purposes. The indoor space exhibits a simple airflow distribution where contaminants are only transported upward, and the DV's boundary layer is influenced solely by the human plume, achieving a stable DV with a high boundary layer height.

During the cooling season (Fig. 1(b)), upward airflow occurs near the high-temperature exterior window glass. This increases the total value of the upward airflow in the room, which risks decreasing the boundary layer height of the DV. However, this influence is considered limited if the ceiling height is sufficient or can be offset by increasing the flow rate of the SA.

However, during the heating season (Fig. 1(c)), DV is challenging to implement because the conditioned supply airflow tends to rise toward the ceiling due to buoyancy. This results in insufficient fresh heating air reaching the occupied areas, decreasing both ventilation and heating efficiency. Additionally, downdrafts often exist near exterior windows or walls during the heating period. These downdrafts disrupt the DV's boundary layer, allowing pollutants from the upper areas of the room to enter and contaminate the occupied space, thereby decreasing the DV's efficiency or destroying its stratification [1,16,17]. This limitation restricts the use of DV in spaces with significant indoor heat loads or minimal need for heating, such as the scenarios introduced above. To broaden the application of DV, current research has focused on three main areas to maintain DV's efficiency for heat supply.

The first approach is to use separate devices for heating or ventilation. A classic combination is DV with radiant heating, such as floor heating [18–21]. Installing radiant panels for spot heating [22] or using the pipe-embedded window [16] are also proposed. However, the increased lifecycle cost for these additional heating devices is a drawback, and the plumes and heat generated from these devices risk disturbing the thermal stratification in the room.

The second approach is to adjust the supply temperature to be close to or cooler than the room air by storing heat during unoccupied periods [23,24], upgrading building insulation [16,25], or using portable units to enhance the DV stratification [26]. These methods are well-designed and have potential for energy saving, but they are still limited by specific usage scenarios and require further examination.

The third approach is to adjust the airflow patterns, such as wall confluent or column attachment ventilation [27–30] that utilize the Coanda effect, supply air with more momentum like impinging jet ventilation [31,32], or using floor-supply DV [33,34] to ensure sufficient air volume reaches the occupied space. While these methods have a similar mechanism to DV and achieve better ventilation performance than traditional mixing ventilation, the increased supply momentum limits their overall efficiency and effectiveness compared to an ideal DV system.

In addition to improving heating performance, further study is warranted on the usage scenarios and air terminals for DV. Regarding use scenarios, ventilation in general hospital wards is considered crucial. Although infectious disease patients are primarily placed in isolation wards, the infection risk in general wards cannot be ignored due to the incubation period or asymptomatic infections [35,36]. Furthermore, unpleasant odors or poor indoor air quality can adversely psychologically and physically impact both patients and visitors [37,38]. However, the application of DV in hospital wards remains controversial and requires further investigation. The main concerns include DV's insufficient elimination of larger bacteria-carrying particles, the creation of high-concentration zones due to thermal stratification locking, and the weak body thermal plume from supine patients, which decreases DV efficiency [39–41]. Contrarily, several studies [42,43] recommend DV for hospital wards, noting that droplets emitted by supine patients tend to accumulate near the ceiling [44], the lock-up effect has minimal impact on the breathing zone [45,46], and the concentrated containment can be further managed with disinfection [47]. Furthermore, DV is sensitive to disturbances caused by occupant activities [48]. The hospital ward typically has less physical activity and changeable heat load, maintaining a more stable DV environment compared to offices or classrooms with high occupant activity levels. Additionally, four-bed wards usually provide sufficient distance between occupants, and cubicle curtains around beds help prevent the spread of particles or droplets.

Regarding the DV air terminal, a prototype all-air wall-mounted induction unit (IU) was considered worthwhile for study. The IU functions similarly to an active chilled beam (ACB) terminal but is an all-air system without a water pipe (details will be introduced in *Section 2.1*). It has energy-saving advantages by inducing room air to mix with the supply air, avoiding the need for reheating, and reducing fan power consumption [49]. Meanwhile, its all-air and low supply velocity design eliminates the condensation and thermal discomfort risk associated with ACB [50,51]. Previous studies [52,53] experimentally examined its performance when ceiling-mounted and showed good performance for cooling, heating, and mixing ventilation. Considering boosting the IU's advantages, particularly its induction mixing characteristics and low supply velocity, our previous studies [45,54] investigated its potential for achieving DV when vertically mounted for cooling usage. Results indicated that stable DV could be achieved by limiting its induction and supply area below the occupied space, with a normalized concentration near the supine patient of less than 0.3. Thermal comfort performance, assessed by draft rate and ADPI, also showed ideal results. However, the all-season performance of this prototype, especially during winter heating, which is a major challenge for DV, has not yet been investigated.

In light of the aforementioned background and gaps in knowledge, this study aims to investigate the ventilation and heating performance of a DV room under winter heating conditions. The method to maintain the ventilation efficiency will be examined and proposed. A four-bed general hospital ward with a vertical wall-mounted induction unit (IU) was chosen for the case study, considering the urgent need for a good indoor environment in wards and to evaluate the IU's winter performance, thereby enriching our ongoing research on this prototype air terminal.

A full-scale experiment will be conducted to assess heating and ventilation performance by evaluating indoor temperature and tracer gas distribution under winter conditions. The influence of near-window downdraft, cubicle curtains, window heaters, and window curtains was also examined to determine the mechanism and efficiency of ventilation during winter.

Without the use of additional heating or air conditioning devices, as illustrated in Fig. 1(d), curtains or partitions were employed to limit air exchange between the near-window and near-bed spaces by restricting airflow through the upper part of the room. This approach prevents near-ceiling contaminants from being entrained by the downdraft and allows the clean downdraft to serve as the supply flow diffusing along the floor, thereby indirectly achieving DV. The usage or the length of the

near-window partition, and the dimension of the cubicle curtain such as ceiling-mounted or on a suspended track, will be adjusted as parameters.

Additionally, numerical studies using CFD analysis were conducted to examine the aforementioned methods under more varied and well-controlled temperature conditions. Extra airflow patterns, such as using local exhaust to boost performance or scenarios where the ceiling-mounted IU performs mixing ventilation, will also be studied and compared. The CFD method will be validated by comparing it to the experimental results. The examination aimed to strengthen the indirect DV theory and evaluate the IU's performance by comparing the numerical results. The infection risk in the ward was also evaluated for reference.

## 2. Experiment setup and parameters

### 2.1. Full-scale laboratory and the wall induction air-conditioning system

The full-scale laboratory simulates a typical Japanese four-bed hospital ward. It is situated on the third floor of a three-story building in Osaka, Japan, and the experiment was conducted during the winters of 2022 and 2023. Fig. 2 provides an overview of the laboratory and its furniture layout, including photographs and detailed geometric dimensions.

The ward, measuring 7000 mm by 7000 mm with a height of 2600 mm, is considered a middle unit in the building that has one exterior surface simulated by an outdoor climate chamber (OCC) on the west side. The other three sides are insulated with 100 mm polystyrene foam (U = 0.22 W/m·K), and the lower floor and ceiling chamber are air-conditioned continuously. The OCC matches the ward's height and length but is 700 mm wide, with a 7 mm styrene board (U = 1.4 W/m$^2$K) and 100 mm polystyrene foam layer to simulate a 10.2 m$^2$ double-layer quartz exterior glass and the wall below it. The air temperature inside the OCC can be controlled to a certain degree by the air conditioner or by introducing outdoor air.

Four hospital beds, each 500 mm in height, are evenly positioned against the walls. Cylinders measuring 1500 mm in length and 300 mm in diameter, covered with black cloth and containing PVC heating cables, are placed on these beds to simulate patients in laying position. Near the beds, four black lamps (incandescent bulbs covered by dark purple glass) are situated 800 mm above the floor to represent equipment heat. The total heat generation in the laboratory is 440 W, with 50 W from each cylinder and 60 W from each black lamp.

Nylon cubicle curtains, 1900 mm long, are suspended from tracks 400 mm below the ceiling and typically closed in a 'U' shape around each bed, with the bottom edge 300 mm above the floor.

Extra equipment and design methods were adjusted as parameters. From the view of mitigating or limiting the down draft near the window, window curtains and window heaters were utilized in some cases (Fig. 2 (a)). As for the window curtain, its nylon materials, 100 mm longer than the window glass and mounted 100 mm away from the window. Three 125 W window heaters are evenly placed on the upper edge of the polystyrene foam windowsill. Each heater consists of four metal fins with special alumite painting to ensure around 0.9 emissivity. The heaters are 1500 mm in length, with a 5 mm gap between each fin and a 10 mm open space between the bottom of the fins and the windowsill.

Moreover, a roll curtain is installed as a partition between the bed and the perimeter space. As shown in Fig. 2(b), the roll curtain is made of a 1 mm transparent vinyl sheet, fixed to the ceiling 1000 mm away from the window, as wide as the ward, and its length $l$ from the ceiling to the bottom edge is variable. Alternatively, the "U"-shaped cubicle curtain can be modified from a suspended track to a ceiling-mounted type by filling the open space between the existing suspended nylon curtain and the ceiling with polycarbonate. A 400 × 360 mm opening facing the ceiling exhaust is maintained to ensure airflow exchange through the cubicle area.

Concerning the air conditioning system, four all-air wall induction units (IUs) are mounted vertically in each corner of the ward, with a 500 × 500 mm exhaust in the ceiling's center. The section and outer view of the wall IU are depicted in Fig. 3. The induction and supply surface of the wall IU is limited to a height of 1040 mm to prevent the induction of contaminants that accumulate above the boundary layer of DV, as determined by the results of our previous study [54]. The primary air (PA) flow rate of the induction units (IUs), which is conditioned air supplied by the air-conditioning system, is set to a total of 607 m$^3$/h (approximately 150 m$^3$/h per unit). This flow rate ensures that the PA is jetted from the 7 mm wide primary air nozzle (Fig. 3(a)) into the induction chamber at a sufficient velocity (approximately 6 m/s in this study) to create the negative pressure that draws in indoor air. This induction and mixing process ensures that the supply air (SA) has a minimal temperature difference from the room air while enabling the use of air with a large temperature difference in the air-conditioning system for power savings. Finally, the mixed SA is supplied into the room at approximately 0.35 m/s through the center perforated panel. The mixing ratio (the proportion of induction air in the SA) varies relative to the PA flow rate and is approximately 0.4 in this study.

The abovementioned velocity data were measured using a hot wire anemometer (details and accuracy are provided in Table 1). The flow rate was verified through calculations based on both the velocity profile and the tracer gas concentration, and was controlled by adjusting the fan speed and air dampers. Further details on the IU's design, mixing ratio, measurement methods, and efficiency for hospital ward DV usage are available in our previous studies [45,54].

### 2.2. Methods and parameters

This study evaluates ventilation and heating performance using steady-state tracer gas and air temperature distribution. Measurements were taken for over 4 h, with data from the final hour averaged for analysis.

The $CO_2$-He tracer gas was emitted from a single patient simulator to represent gaseous or low-density contaminants from an occupant. A 5:3 mixture of $CO_2$ and He gases ($CO_2$ at 1 L/min and He at 0.6 L/min) was used to match the density of air.

Fig. 4 illustrates the arrangement of measurement points. For temperature, 54 T-type thermocouples were distributed across six poles, with nine points per pole vertically. Additionally, 36 thermocouples covered by black aluminum film (emissivity = 0.93) measured surface temperatures, with 12 points on exterior windows and walls, and 24 on the other three walls. Furthermore, the air temperature in the OCC is measured by four thermocouples distributed uniformly throughout the space. Circulator fans are installed inside the OCC to ensure a uniform distribution of temperature. Non-dispersive infrared (NDIR) $CO_2$ gas analyzers, distributed across the same six poles, measured tracer gas concentration at six vertical points per pole, totaling 36 points. The temperature and concentration of both primary air (PA) and exhaust air (EA) were also recorded. All the data were recorded at 30-s intervals. Details and accuracy of the measurement equipment are listed in Table 1.

Table 2 presents the number and specific parameters for each experimental case. Cases Exp1-4 aim to examine the IU's heating and ventilation performance and explore the impact of the window heater and curtain in mitigating or limiting downdraft. One case without the cubicle curtain was also investigated. These four cases were conducted in February 2023. The air temperature difference ($\Delta\theta$) between the OCC's interior and the average air temperature at a height of 1.1 m inside the ward was adjusted to approximately 15 °C to represent the indoor-outdoor temperature difference in Osaka, Japan. Due to the insufficient cooling power of the OCC, the indoor air temperature was set higher than usual heating scenarios (around 30 °C) to ensure the $\Delta\theta$ was close to 15 °C.

Cases Exp5-16, conducted in February and March 2024, investigated whether a roll curtain at the perimeter or a ceiling-mounted cubicle

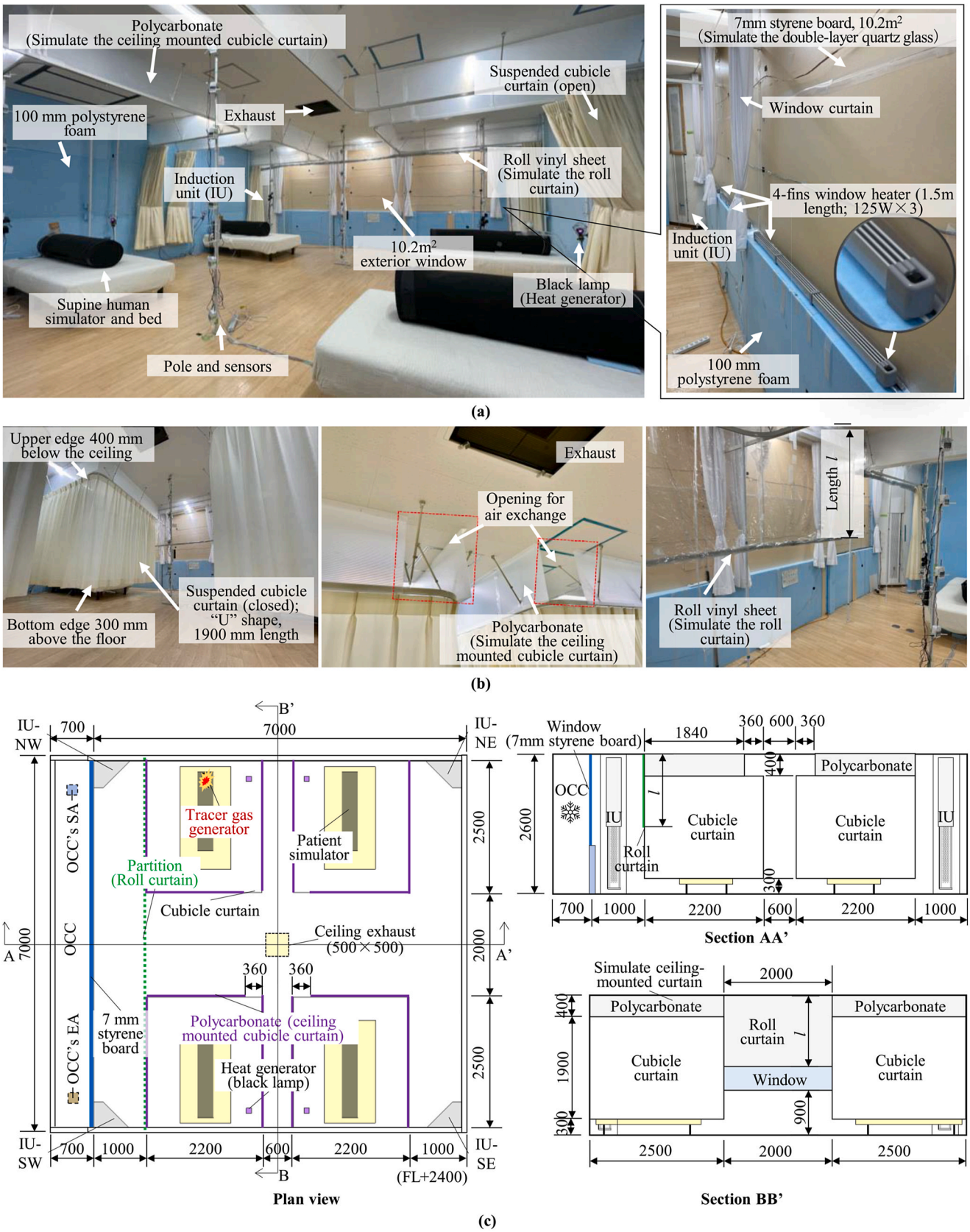


**Fig. 2.** Image of the full-scale four-bed ward laboratory with all-air induction unit (IU) for displacement ventilation, elements and design to improve ventilation efficiency during winter; (a) photograph of the laboratory and the simulated exterior window; (b) suspended and ceiling-mounted cubicle curtain around the beds, roll curtain in the perimeter; (c) section and exterior view of the wall IU.

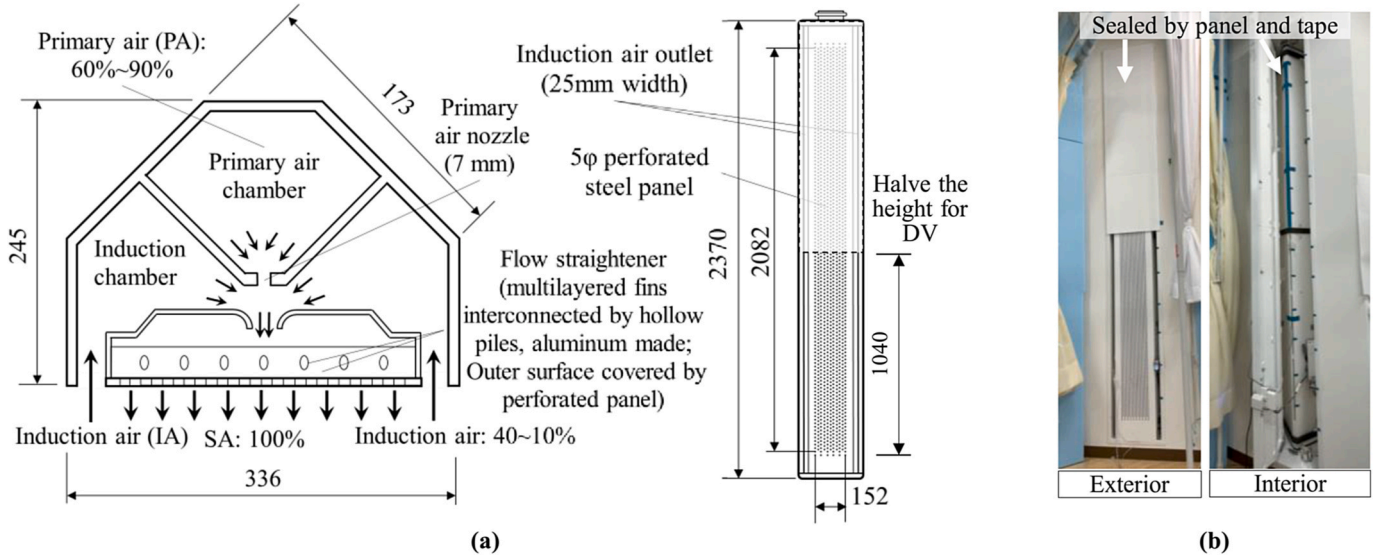


**Fig. 3.** The all-air wall induction unit (IU) used for ward displacement ventilation (DV). (a) section and exterior geometric dimensions of the IU; (b) photographs of the IU in the ward laboratory.

**Table 1**
Details and accuracy of the experimental devices.

| Usage | Model name | Manufacturer | Range or condition | Accuracy |
|---|---|---|---|---|
| Temperature measurement | T type, 0.32 mm | Ninomiya Co., Ltd. | −40°C- 90 °C | ASTM E230 Standard class |
| Temperature data logger | CADAC3 | Etodenki Corporation | 0- 10 KHz | 0.01 °C |
| $CO_2$ concentration measurement | TR-576 | T&D Corporation | 0 to 9999 ppm | ±(50 ppm +5 % of reading) at 5000 ppm or less; further calibrated by the span gas |
| $CO_2$ flow rate controller | FCS1030LC-F10L-CO2 | Fujikin | 0–10 L/min | ±1 % F.S. (at 15–35 °C) |
| Velocity measurement | Model 6501 with 6551-21 probe | KANOMAX | 1.1–30.0 m/s | ±2.0 % of reading or 0.02 m/s |

curtain could improve ventilation efficiency by limiting contaminants' horizontal movement and affecting airflow distribution. Due to the warm winter in East Asia that year, the OCC's air temperature could only be cooled to around 18 °C. Therefore, the maximum $\Delta\theta$ for these cases was controlled to be around 12 °C.

Cases Exp5-8 examined the influence of the perimeter roll curtain length $l$ A suspended cubicle curtain with a 400 mm gap near the ceiling was placed around the beds. The roll curtain lengths were varied as follows: 0 mm (not used), 400 mm, 1250 mm, and 2300 mm.

Cases Exp9-12 tested the performance of using the ceiling-mounted cubicle curtain alone or combined with roll curtains of 400 mm, 1250 mm, and 2300 mm lengths.

Cases Exp13-16 used the same curtains arrangement as cases 9–12 but changed the $\Delta\theta$ from around 12 °C to around 5 °C to investigate the influence of temperature difference.

The average PA temperature ($\theta_{PA}$) of the four IUs and the air temperature inside the OCC are also shown in Table 2 for reference.

## 3. Computational setup and numerical scheme

Steady-state CFD analysis was conducted to further investigate various temperature conditions and airflow patterns under well-controlled settings. Initially, several experimental conditions were replicated to validate the CFD model. Subsequently, scenarios that were not experimentally explored, such as combinations with local exhaust systems or the use of ceiling-mounted air conditioning units, were analyzed and compared. Additionally, the window heat loss was adjusted over a wide range to examine its influence.

### 3.1. Laboratory 3D models and simulation parameters

The 3D models of the four-bed ward, which match the laboratory's dimensions and layout but omits the OCC are shows in Fig. 5. The parameters and abbreviations for each CFD analysis case are summarized in Table 3.

The examination of the window heater and window curtain is omitted, as the experimental study clearly demonstrated their effects. Comparisons among suspended and ceiling-mounted cubicle curtains, perimeter roll curtains of different lengths, and changing the IU from wall-mounted to ceiling-mounted, as well as combining the wall IU with local exhausts, were conducted with a fixed window heat loss condition (125 W/m$^2$, CFD1-5)). Additionally, the impact of varying window heat losses (0–150 W/m$^2$, CFD6-12)) was assessed under the same curtain layout and airflow pattern.

Fig. 5*(a)* depicts the standard condition, representing the normal setup of a four-bed ward with suspended cubicle curtains around the hospital beds and corner vertical mount IUs for DV.

Fig. 5*(b)* shows the additional use of the perimeter roll curtain. Apart from the cases for validation usage, the length $l$ of the roll curtain is fixed at 800 mm as experiments showed no significant difference with lengths of 400 mm, 1250 mm, or 2300 mm (discussed in the next section). The 800 mm roll curtain ensures an 1800 mm height open space below, balancing containment-blocking performance and practical considerations.

Fig. 5(c) shows the use of the ceiling-mounted cubicle curtain around the beds. Similar to the experiment, a 360 × 400mm opening facing the ceiling center exhaust is left to ensure airflow exchange inside and outside the cubicle area.

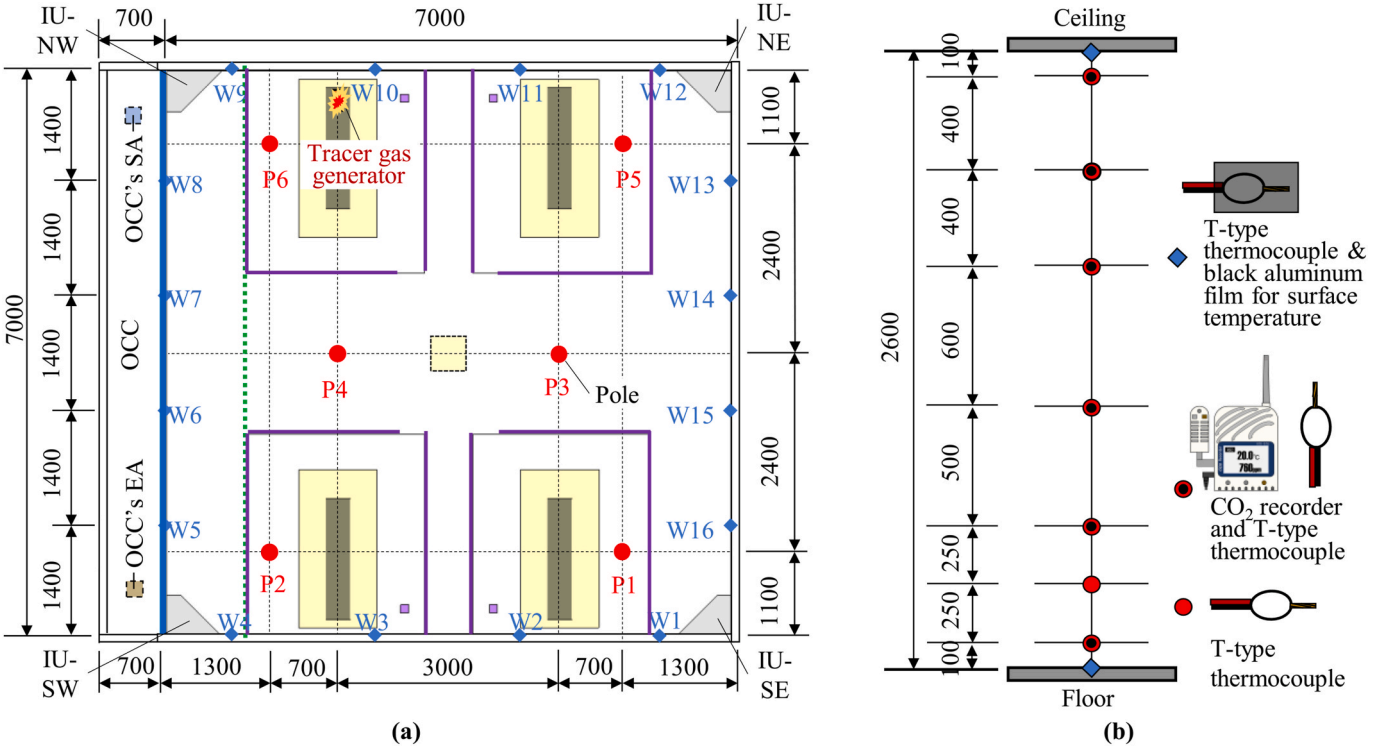


**Fig. 4.** Arrangement of the measurement points. (a) Horizontal distribution in the labotrary; (b) vertical distribution on a single pole.

**Table 2**
Parameters of the full-scale experiment.

| Parameters | | | | | | Reference | | |
|---|---|---|---|---|---|---|---|---|
| Case | Parameter abbreviation | "U" shape Cubicle Curtain | Window curtain or heater | Roll curtain and its length $l$ (mm) | $\Delta\theta$ (°C) | $\theta_{PA}$ (°C) | OCC air (°C) | EA (°C) |
| Exp1 | NC-(15)-R0 | Not used | Not used | Not used (0) | 14.77 | 32.38 | 11.93 | 27.48 |
| Exp2 | UC-(15)-R0 | Suspended mount (UC) | | | 14.46 | 33.60 | 12.59 | 28.27 |
| Exp3 | UWC-(15)-R0 | | Window curtain | | 14.30 | 39.73 | 15.49 | 31.21 |
| Exp4 | UWCH-(15)-R0 | | Window curtain and heater | | 14.61 | 39.38 | 14.76 | 30.69 |
| Exp5 | UC-(12)-R0 | Suspended mount (UC) | Not used | Not used (0) | 11.94 | 39.62 | 19.17 | 30.38 |
| Exp6 | UC-(12)-R400 | | | 400 | 11.00 | 39.51 | 17.16 | 30.24 |
| Exp7 | UC-(12)-R1250 | | | 1250 | 11.18 | 39.94 | 18.27 | 31.06 |
| Exp8 | UC-(12)-R2300 | | | 2300 | 12.32 | 39.47 | 17.47 | 30.97 |
| Exp9 | UCC-(12)-R0 | Ceiling Mount (Polycarbonate blocking curtain's upper opening, UCC) | Not used | Not used (0) | 11.11 | 40.95 | 19.06 | 32.10 |
| Exp10 | UCC-(12)-R400 | | | 400 | 12.14 | 41.27 | 19.08 | 33.08 |
| Exp11 | UCC-(12)-R1250 | | | 1250 | 11.81 | 41.93 | 19.04 | 33.67 |
| Exp12 | UCC-(12)-R2300 | | | 2300 | 11.30 | 40.79 | 18.37 | 31.14 |
| Exp13 | UCC-(5)-R0 | Ceiling Mount (Polycarbonate blocking curtain's upper opening, UCC) | Not used | Not used (0) | 4.10 | 23.41 | 18.27 | 22.00 |
| Exp14 | UCC-(5)-R400 | | | 400 | 5.11 | 23.06 | 17.60 | 23.07 |
| Exp15 | UCC-(5)-R1250 | | | 1250 | 4.96 | 23.79 | 17.93 | 23.19 |
| Exp16 | UCC-(5)-R2300 | | | 2300 | 4.47 | 25.83 | 18.73 | 23.46 |

*Abbreviation naming convention: XX-(00)-R0000.
XX: Denotes the type of equipment or fixture, such as cubicle curtain, window curtain, or heater.
(00) represents the temperature difference $\Delta\theta$ between the OCC and the indoor air at 1.1m height above the floor (°C).
R0000: Indicates the length $l$ of the roll curtain.

Fig. 5(d) shows the combined use of the perimeter roll curtain and ceiling-mounted cubicle curtain. The roll curtain primarily aims to stop the horizontal movement of contaminants in the room center, which is outside the cubicle curtain's range.

Fig. 5*(e)* has the same curtain arrangement as the standard condition (Fig. 5(a)) but changes the ceiling center exhaust to four local exhausts directly above the beds. Each exhaust has a uniform outlet volume.

Fig. 5*(f)* has the same curtain arrangement as the standard condition

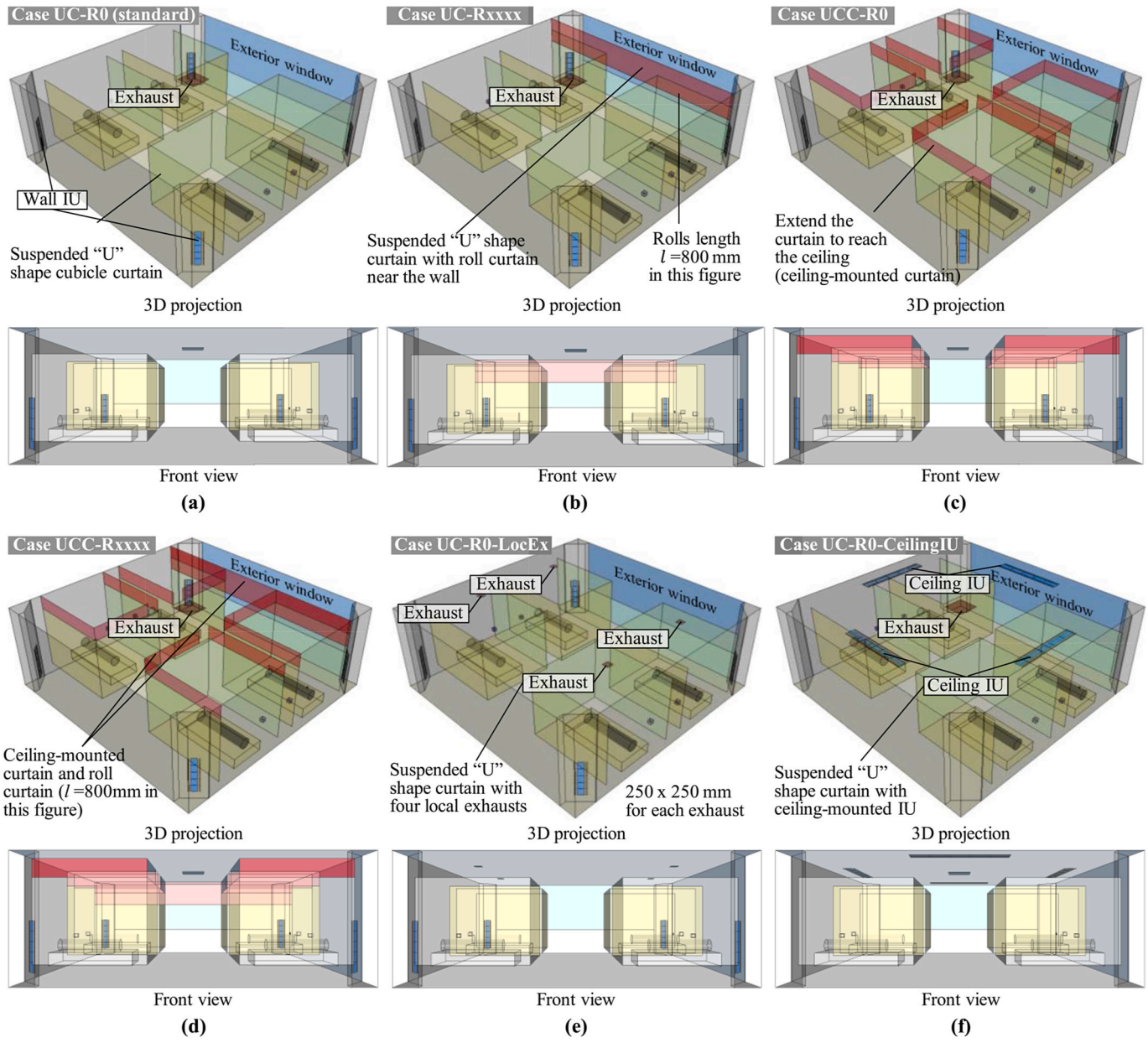


**Fig. 5.** 3D models and parameters of the CFD numerical study. (a) standard four-bed ward with suspended cubicle curtains; (b) addition of a ceiling-mount roll curtain 1m away from the window; (c) extend the suspended cubicle curtain to ceiling-mount, leaving an opening facing the exhaust; (d) combination of ceiling-mount cubicle curtain and roll curtain; (e) central ceiling exhaust replaced with four local exhausts above the beds; (f) ward with ceiling-mount induction units (IU).

(Fig. 5(a)) but replaces the wall-mounted IUs with ceiling-mounted units, aiming to evaluate the differences between DV and MV for winter usage.

As summarized in Table 3, the first four cases (CFD-Exp 9,12,13,16) are for CFD validation purposes, considering they are involving the use of a ceiling-mounted cubicle curtain, with or without a 2300 mm roll curtain, and temperature differences ($\Delta\theta$) of 5 °C and 12 °C. While cases CFD1 to CFD12 are for the further numerical study. Temperature boundary conditions are provided for reference. The validation cases mirror the experimental conditions by using defined temperature data, while the numerical study cases employ fixed temperature or heat generation settings. Details about the CFD setup will be introduced in the next section.

### 3.2. CFD setup and data processing

Commercial software Cradle scSTREAM V2022 (Hexagon AB) is used for the CFD study. Details regarding the CFD settings are summarized in Table 4 for the analysis methods and Table 5 for the boundary conditions. The CFD methods for the IU and four-bed ward, including the turbulence models, meshing method impact, heat transfer settings, and flow or velocity properties of the IU, have been proposed, examined, and validated in our previous work [45,54]. This study employs similar CFD setups to those in our previous work, and they are briefly introduced as follows.

The standard k-epsilon (SKE) model was chosen for turbulence analysis, as it provides similar accuracy to the RNG k-epsilon model and linear low-Reynolds model for ward ventilation simulation. The overall grid design for the standard condition (case CFD-1) is shown in Fig. 6(a), with detailed views of the grid near the window or wall surface presented in Fig. 6(b). The mean y + at the window surface for each case is summarized in Fig. 6(c). The first grid from the wall and window surface has a thickness of 150 mm to ensure the log-law region is at a non-dimensional length y + greater than 30 from the wall.

**Table 3**
Case number, abbreviation, and parameters of the CFD simulation.

| Case | Parameter abbreviation | Cubicle curtain | Roll curtain's length $l$ (mm) | SA and EA's location | Window inner surface (°C or W/m$^2$)) | PA (°C) | Floor surface (°C) | Ceiling surface (°C) | Wall (°C) |
|---|---|---|---|---|---|---|---|---|---|
| CFD-Exp9 | UCC-(12)-R0-Exp | Ceiling-mounted | 0 | Corner IU and center exhaust | 27.65 °C | 40.95 | 26.18 | 28.60 | 29.65 |
| CFD-Exp12 | UCC-(12)-R2300-Exp | | 2300 | | 28.42 °C | 40.79 | 24.93 | 28.11 | 29.35 |
| CFD-Exp13 | UCC-(5)-R0-Exp | | 0 | | 20.78 °C | 23.41 | 21.06 | 22.72 | 21.66 |
| CFD-Exp16 | UCC-(5)-R2300-Exp | | 2300 | | 22.04 °C | 25.83 | 21.42 | 22.05 | 23.00 |
| CFD-1 | UC-(125 W)-R0 | Suspended | 0 | Corner IU and center exhaust | −125 W/m$^2$ | 26 | 24 | 26 | Adiabatic outer surface (inner surface not specified) |
| CFD-2 | UC-(125 W)-R800 | | 800 | | | | | | |
| CFD-3 | UC-(125 W)-R0-LocE | | 0 | Corner IU and local exhaust | | | | | |
| CFD-4 | UC-(125 W)-R0-CeiIU) | | | Ceiling IU and center exhaust | | | | | |
| CFD-5 | UCC-(125 W)-R0 | Ceiling-mounted | 0 | Corner IU and center exhaust | −125 W/m$^2$ | | | | |
| CFD-6 | UCC-(0 W)-R800 | | 800 | | 0 | | | | |
| CFD-7 | UCC-(25 W)-R800 | | | | −25 W/m$^2$ | | | | |
| CFD-8 | UCC-(50 W)-R800 | | | | −50 W/m$^2$ | | | | |
| CFD-9 | UCC-(75 W)-R800 | | | | −75 W/m$^2$ | | | | |
| CFD-10 | UCC-(100 W)-R800 | | | | −100 W/m$^2$ | | | | |
| CFD-11 | UCC-(125 W)-R800 | | | | −125 W/m$^2$ | | | | |
| CFD-12 | UCC-(150 W)-R800 | | | | −150 W/m$^2$ | | | | |

*Abbreviation naming convention: XX-(00)-R0000.
XX: Denotes the type of equipment or fixture, such as cubicle curtain, window curtain, or heater.
(00) represents the temperature difference $\Delta\theta$ between the OCC and the indoor air at 1.1m height above the floor (°C); or the heat loss from the window surface per square meter (W/m$^2$).
R0000: Indicates the length $l$ of the roll curtain.

**Table 4**
CFD meshing and calculation settings.

| CFD code | Cradle scSTREAM V2022, Hexagon AB |
|---|---|
| Turbulence Model | Standard $k$-$\varepsilon$ (SKE) model |
| Algorithm | SIMPLE |
| Discretization Scheme | QUICK |
| Radiation analysis | View Factor method |
| Number of calculation cycle | 10,000 |
| Residuals | Less than $1x10^{-5}$ |
| Standard grid size | 50 mm |
| Standard geometric ratio | 1.1× |
| Number of grids | Around 3,000,000 |
| First grid from the wall | 150-mm thickness |

The entire analysis space used a structured grid. Near the cylindrical human simulator, a fine grid with a width of 15 mm was applied to accurately capture the shape of the cylindrical elements. While this approach may pose risks in ensuring the accuracy of heat transfer predictions, the surface temperature of the cylinder was accurately predicted when compared with experimental data and the results of the low-Reynolds model simulations. Considering the study's focus on indoor temperature and airflow simulation, this limitation is expected to have minimal impact on the overall accuracy.

Radiation analysis was conducted using the view factor method. The convection heat transfer coefficient of the inner surface of the walls and windows was calculated based on ASHRAE data, with the radiation effect removed. The validation cases mirror the experimental conditions by defining the primary air (PA), wall, and window surface temperatures according to the measurement results (summarized in Table 3). In contrast, the numerical study cases fixed the floor and ceiling surface temperatures at 24 °C and 26 °C, respectively, and maintained the PA air temperature at 26 °C. Heat loss from the OCC (exterior window) was simulated by specifying the value in watts.

Fig. 7 illustrates the airflow boundaries designed to replicate the IU's induction and mixing air supply properties. This method was proposed and verified in our previous study [54], and is briefly introduced below.

The setup uses two groups of outlet boundaries and one group of inlet boundaries to reproduce the IU's induction and supply properties. Each group is divided into five vertical sections to account for temperature and concentration gradients. Each airflow boundary has unique velocity properties, calculated based on the PA volume, PA's velocity distribution, IU's mixing ratio, and the boundary dimensions. Monitoring points $P_i$ in the center of each induction (outlet) boundary track temperature ($T_{IA}$) and concentration ($C_{IA}$) data per calculation cycle. The following functions calculate the temperature ($T_{SA}$) and concentration ($C_{SA}$) of the IU's supplied air, with $T_{PA}$ as the temperature of the PA supplied by the air-conditioning units and $R_{mix}$ as the IU's mixing ratio (0.4).

$$T_{SA} = (1 - R_{mix}) \times T_{PA} + R_{mix} \times T_{IA} \quad (1)$$

$$C_{SA} = (1 - R_{mix}) \times C_{PA} + R_{mix} \times C_{IA} \quad (2)$$

For data processing, CFD validation data was collected from the same locations as in the laboratory. In the numerical study (Fig. 8*(a)*), temperature and concentration vertical distributions were evaluated in five areas: Areas 1–4 within the cubicle curtain and Area 5 at the ward's center. CFD results were collected at a 10 × 10 cm resolution, and the mean value from the same height in each area was used for analysis.

As shown in Fig. 8*(b)*, a space measuring 500 mm in length, 970 mm in width, and 400 mm in height at the end of the bed represents the breathing area of a supine patient. The mean normalized concentration in each breathing area is used to calculate the infection probability for the patients.

The infection probability for the other three patients, away from the infected individual, is evaluated using the Wells-Riley model, as shown in the following equation:

$$p = 1 - e^{-n} \quad (3)$$

**Table 5**
Summary of the CFD boundary settings.

| | | | |
|---|---|---|---|
| Wall | Wall boundary | | No-slip |
| | Outer surface | | Adiabatic |
| | Inner surface (Specifying heat transfer coefficient) | Wall | 3.06 W/m$^2$·k; Temperature matching experimental data or not specified |
| | | Window | 3.06 W/m$^2$·k; Temperature matching experimental data or specified heat generation (W/m$^2$); Table 3 |
| | | Floor | 0.97 W/m$^2$·k; Temperature matching experimental data or fixed = 24 °C |
| | | Ceiling | 4.04 W/m$^2$·k; Temperature matching experimental data or fixed = 26 °C |
| Radiation boundary | Specifying emissivity | | All solid surfaces; Emissivity = 0.9 |
| Curtain | "U" shape cubicle curtain | Top | 400 mm free space or 0 (ceiling-mounted) |
| | | Central | 1900- or 2300-mm length panel, with a 360 × 400 mm opening facing the exhaust when mounted on the ceiling |
| | | Lower | 300 mm free space |
| | Roll curtain | Ceiling-mounted, 1m away from the window | Length $l$ = 0, 800, 2300 mm |
| Flow boundary | Air-conditioning systems | IU's inlet | Specific volume and temperature |
| | | IU's outlet | Specific volume |
| | | Temperature and concentration | Calculate by mixing ratio |
| | | Exhaust | Natural outflow; Central exhaust: 500 × 500 mm, Local exhaust: 250 × 250mm × 4 |
| | Tracer gas | Physical properties | Diffusion coefficient: $1.39 \times 10^{-5}$ (m$^2$/s) [55] for $CO_2$-Air. Density etc., are equal to air |
| | | Flow rate | 1.5 L/min, volume specify |
| | | Generation temperature | Matching the experimental data, or fixed = 34 °C |
| | | Diffusion area & direction | 25 × 25 mm square, upward |
| Inlet's turbulence statistics | Turbulence intensity $I$ and length scale | | Specified $I$ = 1 % and length scale = 5 mm |
| | Kinetic energy $k$ and dissipation rate $\varepsilon$ | | Calculated by $u$, $I$, and length scale |
| Occupants and equipment heat | Patient simulator | Heat generation | 50 W × 4, volumetrics heat source |
| | | Dimension | 1500 mm (L) × 300 (Φ) cylinder × 4 |
| | Equipment heat load | Heat generation | 60 W × 4, volumetrics heat source |
| | | Dimension | 100 mm cube × 4 |

where $p$ is the probability of infection, and $n$ is the quanta inhaled, calculated based on the normalized concentration using the following equation.

$$n = \frac{q}{Q} \cdot C^*_{inhale} \cdot Q_b \cdot D \quad (4)$$

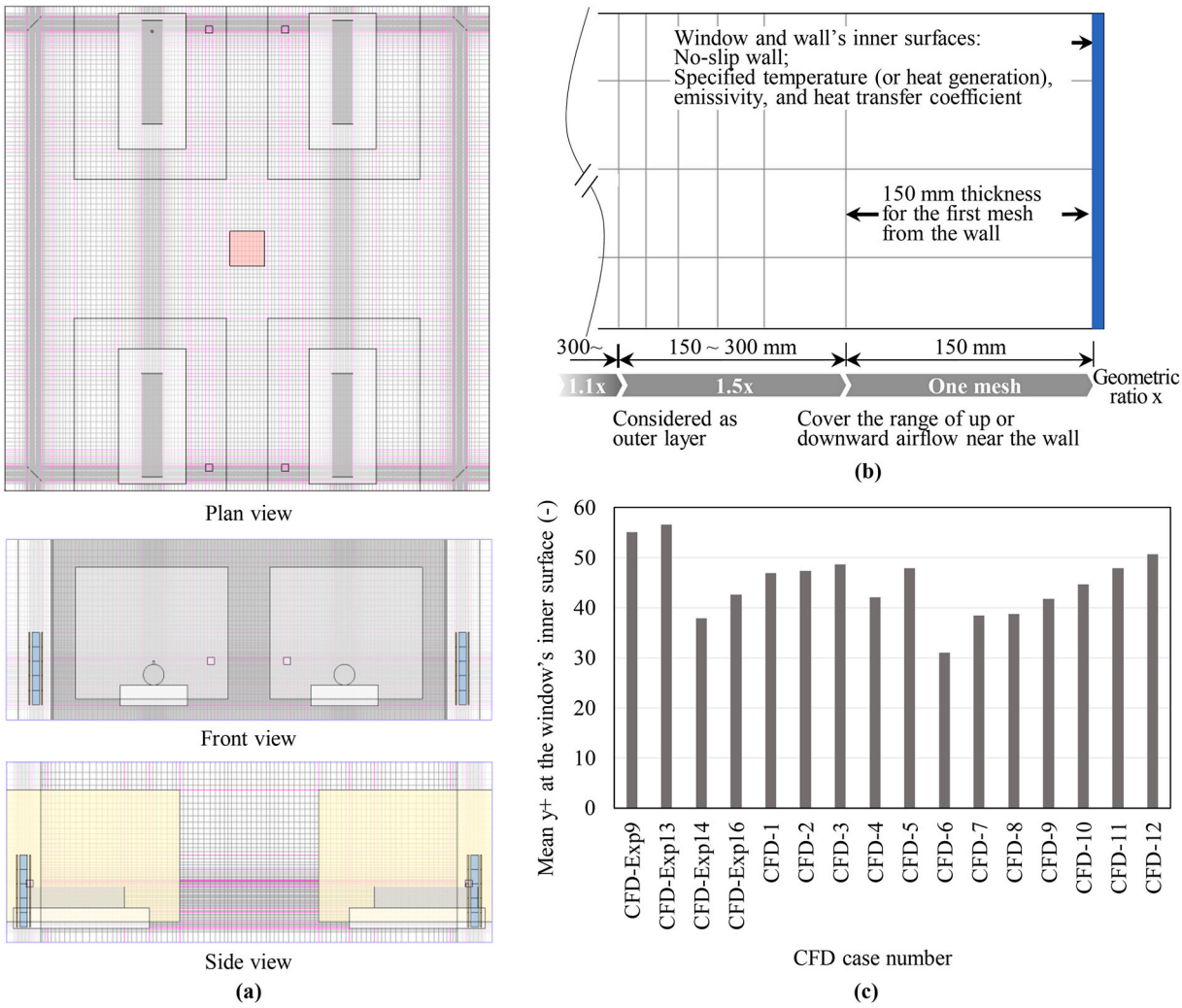


**Fig. 6.** Grid design of the four-bed ward and non-dimensional length y + at the window surface for reference (a) grid design of the standard condition (case CFD-1) shown through three views as an example; (b) grid design near wall or window surfaces; (c) mean y + at the window surface of each CFD case.

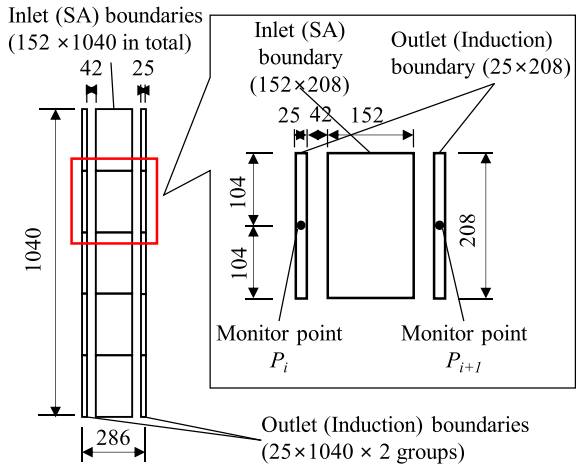


**Fig. 7.** Airflow boundaries to reproduce the IU's induct and mixing air supply properties.

In this equation, $q$ is the quanta emission rate of the infected individual, defined as 3.14 quanta/h for resting and oral breathing activity based on the REHVA guidebook [56]. $Q$ is the room's ventilation rate (607 $m^3$/h). $Q_b$ is the occupant's breathing rate defined as 0.54 $m^3$/h for "standing" (not talking and exercising) activity [56]. $C^*_{inhale}$ is the normalized concentration inhaled.

The duration $D$ is based on the COVID-19 incubation period, chosen as five days (120 h) [57,58] for this study because the actual duration of the patient's stay is difficult to quantify.

## 4. Results and discussion

The normalized concentration $C_n$ was used to evaluate the ventilation performance in the ward and is calculated using the following equation.

$$C_n = \frac{C_P - C_{PA}}{C_{EA} - C_{PA}} \tag{5}$$

where $C_p$ represents the concentration at the sampling point, $C_{PA}$ represents the concentration of the IU's primary air (PA), and $C_{EA}$ represents the concentration of the exhausted air. In the CFD analysis, $C_{PA}$ was set to 0 as return air was not considered.

The experimental data compares vertical temperature distribution in two groups: the average values at identical heights on P1, P2, and P5 (near the beds) and P3 and P4 (room's center). The vertical distribution of normalized concentration is averaged in three groups: P6 (near the generation source), P3 and P4 (room's center), and P5 and P6 (near

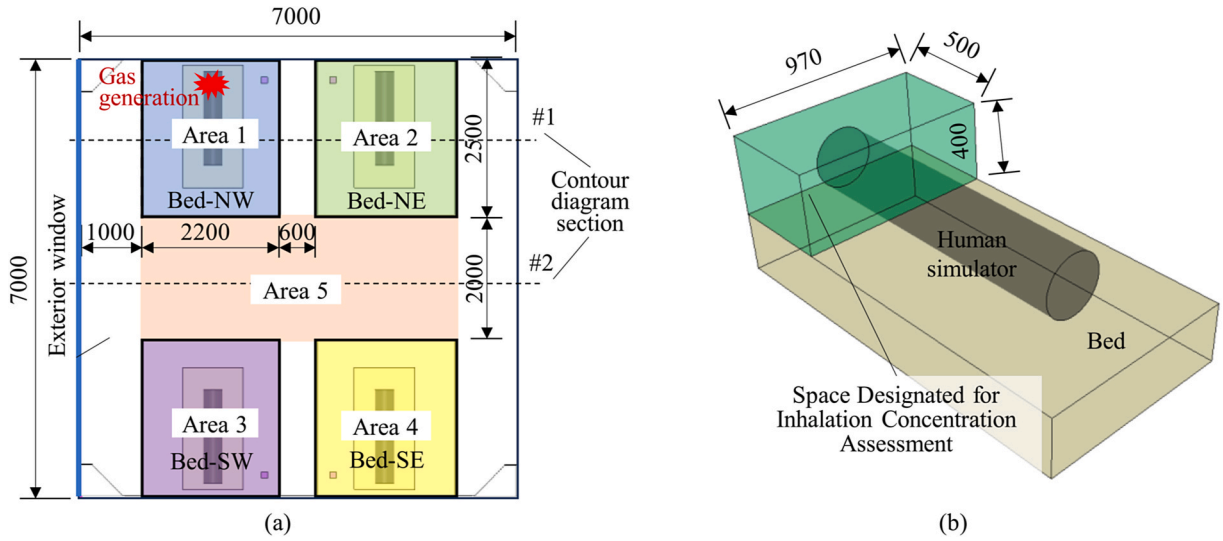


**Fig. 8.** Dimensions of the sections and areas defined for data collection. (a) Areas and sections used to evaluate the vertical distribution of temperature and concentration.; (b) space defined as the breathing area of an occupant lying on a hospital bed.

other beds away from the source).

### 4.1. Full-scale experiment

#### 4.1.1. Ventilation mechanism during heating and improving method by eliminating down draft

Fig. 9 showcases the experimental outcomes for cases Exp1 through Exp4. The comparison includes the effects of having the suspended cubicle curtain open (NC) or closed (UC), the additional use of the window curtain (UWC), or both the curtain and heater (UWCH) on temperature and concentration distribution. The temperature differential ($\Delta\theta$) between the OCC and the room's air temperature at a height of 1.1 m is around 15 °C.

For temperature distribution, due to the OCC's insufficient cooling power and the laboratory not being fully adiabatic, cases UWC and UWCH have a higher PA temperature (around 39.5 °C) compared to UC and NC (around 33 °C) to maintain a $\Delta\theta$ of approximately 15 °C. This results in an approximate 2 °C difference between the two groups, as shown in Fig. 9*(a)*. However, all four cases exhibit a similar vertical temperature gradient, with a 2–3 °C difference in the occupied zone, which has limited influence on thermal comfort and is appropriate for achieving DV. No significant differences were found in the impact of curtains and heaters on temperature distribution.

Regarding the concentration distribution, case NC has the least ideal results, especially in the space away from the generation source. The normalized concentration at 0.1–0.6 m above the floor is around 1, while near the ceiling, it is around 0.7. This indicates that the tracer gas is falling and diffusing along the floor. Near the generation source, there is no vertical gradient and the concentration is the lowest compared to other cases, showing that DV is not achieved and contaminant diffusion is uncontrolled. The likely reason is that, without the cubicle curtain's block, the tracer gas was entrained by the downdraft near the window or disturbed by the IU's supply air before rising to the upper area of the room.

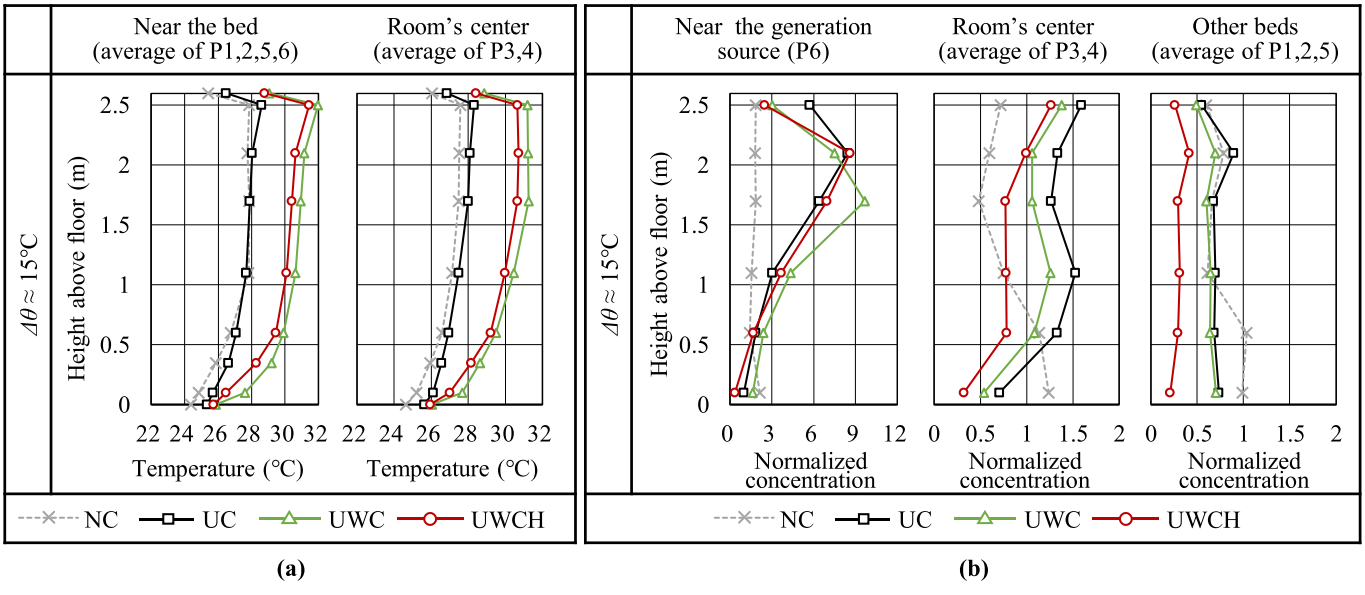


**Fig. 9.** Experimental results of heating and ventilation performance comparison when using the suspended cubicle curtain (UC) or not (NC), window curtain (UWC), and window heater (UWCH) (a) temperature vertical distribution. (b) Normalized concentration vertical distribution.

When keeping the cubicle curtain around the bed closed (case UC), the normalized concentration increases compared to case NC but shows a vertical gradient more similar to DV, with lower concentrations at 0.1–0.6 m above the floor. The normalized concentration around the other hospital beds decreases to less than 0.7. In the room's center, the highest concentration shifts from near the floor to about 1 m above the floor, indicating a decrease in tracer gas entrainment by the downdraft and diffusion along the floor. The cubicle curtain around the generation source limits the gas's horizontal movement, concentrating most of it within the cubicle curtain's range and achieving an airflow pattern more similar to DV.

Cases UC and UWC show similar concentration distributions across all measurement points. Closing the window curtain does not effectively limit down draft or tracer gas entrainment, and thus does not significantly improve ventilation performance.

In case UWCH, which uses window heaters with the cubicle curtain closed, a DV concentration gradient is observed in the room's center. This case has the lowest concentration near the bed away from the generation source (around 0.3). The window heater eliminates the downdraft near the window, allowing the tracer gas to rise to the near-ceiling space, and possibly accelerating it through the upward airflow generated by the heater.

It can be concluded that downdrafts can significantly weaken or disrupt DV's ventilation performance. Using a window heater to eliminate downdrafts prevents contaminants from being entrained downward, ensuring the normalized concentration near other beds remains around 0.3 in this study. Although ventilation performance may still be weaker compared to cooling supply conditions, this is likely because the clear air supplied to the occupied zone during heating is less than during cooling due to buoyancy effects.

Additionally, using a cubicle curtain around the generation source improves normalized concentration results (0.8 near other beds) compared to an open curtain, with a concentration gradient similar to DV. This distribution is not entirely achieved by direct airflow from the supply vents as in cooling conditions. During winter heating, some of the clean supply air initially rises near the ceiling due to buoyancy and, before being affected by pollutants, is entrained by the down draft and supplied to the occupied zone. However, the down draft also entrains contaminants downward. This results in a concentration distribution with a DV-like vertical gradient but inferior cleanliness in the occupied zone and higher concentration at the room's center height, which can be described as a "quasi-displacement ventilation" scenario. Therefore, the next section will focus on methods to improve this by limiting the horizontal diffusion of contaminants through the redesign or addition of curtains or partitions to ensure the cleanliness of the down draft.

#### 4.1.2. *Improvement method by limiting the containment horizontal diffusion*

The case with suspended cubicle curtains around the beds but no curtains or heaters near the window (UC-R0) was defined as the basic condition. Fig. 10 shows the experimental results when a roll curtain was added on the ceiling 1000 mm from the window. The length of the roll curtain (400 mm, 1250 mm, 2300 mm) was adjusted to investigate its influence. Fig. 11 presents similar cases to Fig. 10 but changes the suspended cubicle curtains to ceiling mounted. The results of the basic condition are also shown in Figs. 10 and 11 for comparison.

For the temperature difference $\Delta\theta$, 12 °C was aimed for in these cases (as introduced in Section 2.2). Additionally, experiment results under a smaller $\Delta\theta$ of 5 °C when using the ceiling-mounted curtain are shown in Fig. 11 for further comparison.

Regarding temperature distribution, the presence or length of the roll curtain does not significantly influence the results. However, the ceiling-mounted curtain increases the vertical temperature difference in the room's center (Fig. 11, $\Delta\theta$ = 12 °C), resulting in a uniform vertical temperature distribution above 1.1m height near the bed, but with an around 1.5 °C difference in the room's center. This suggests that the ceiling-mounted curtain restricts airflow exchange between the inside and outside of the cubicle area around the beds.

Regarding concentration distribution, as shown in Fig. 10, when using the suspended cubicle curtain around the bed, the presence of the perimeter roll curtain decreases the normalized concentration in the space away from the generation source from around 0.8 to around 0.5. Additionally, the longer the roll curtain, the more the normalized concentration tends to decrease.

Changing the suspended cubicle curtain to ceiling mounted further reduces the normalized concentration near other beds to mostly less than 0.5, even without the combined use of the perimeter roll curtain (upper part of Fig. 11). Combining the ceiling-mounted curtain with the perimeter roll curtain and selecting a longer curtain can further decrease the normalized concentration, but this trend is not very significant, and using the longest roll curtain ($l$ = 2300 mm) may have the opposite effect.

When the $\Delta\theta$ is around 5 °C (bottom part of Fig. 10), all cases exhibit ideal ventilation performance, with normalized concentration in most of

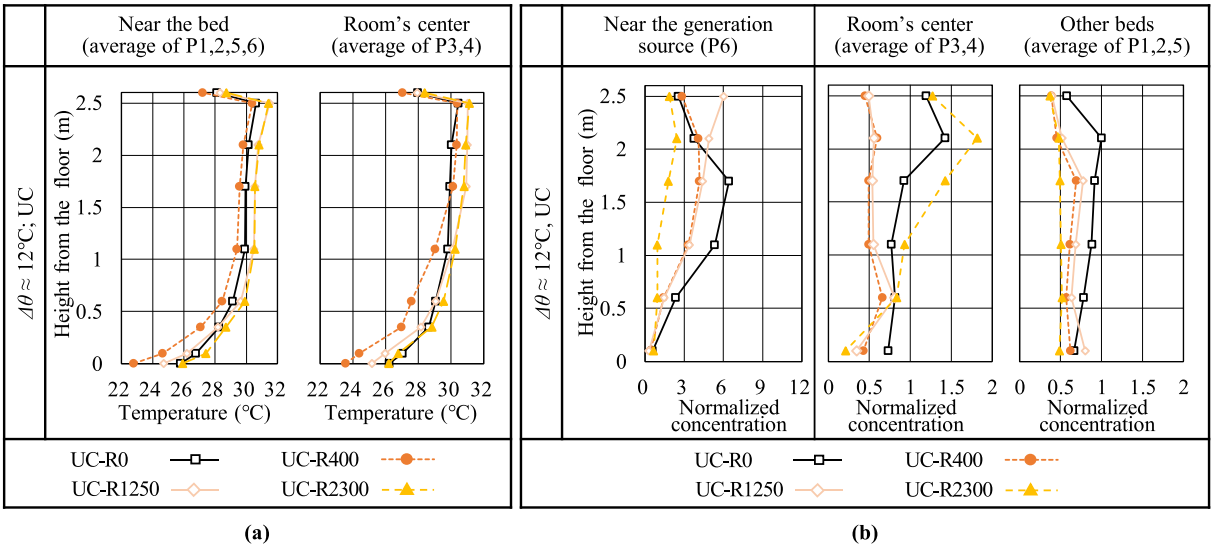


**Fig. 10.** Experimental results of heating and ventilation performance comparison regarding the presence and length of the perimeter roll curtain (a) temperature vertical distribution; (b) normalized concentration vertical distribution.

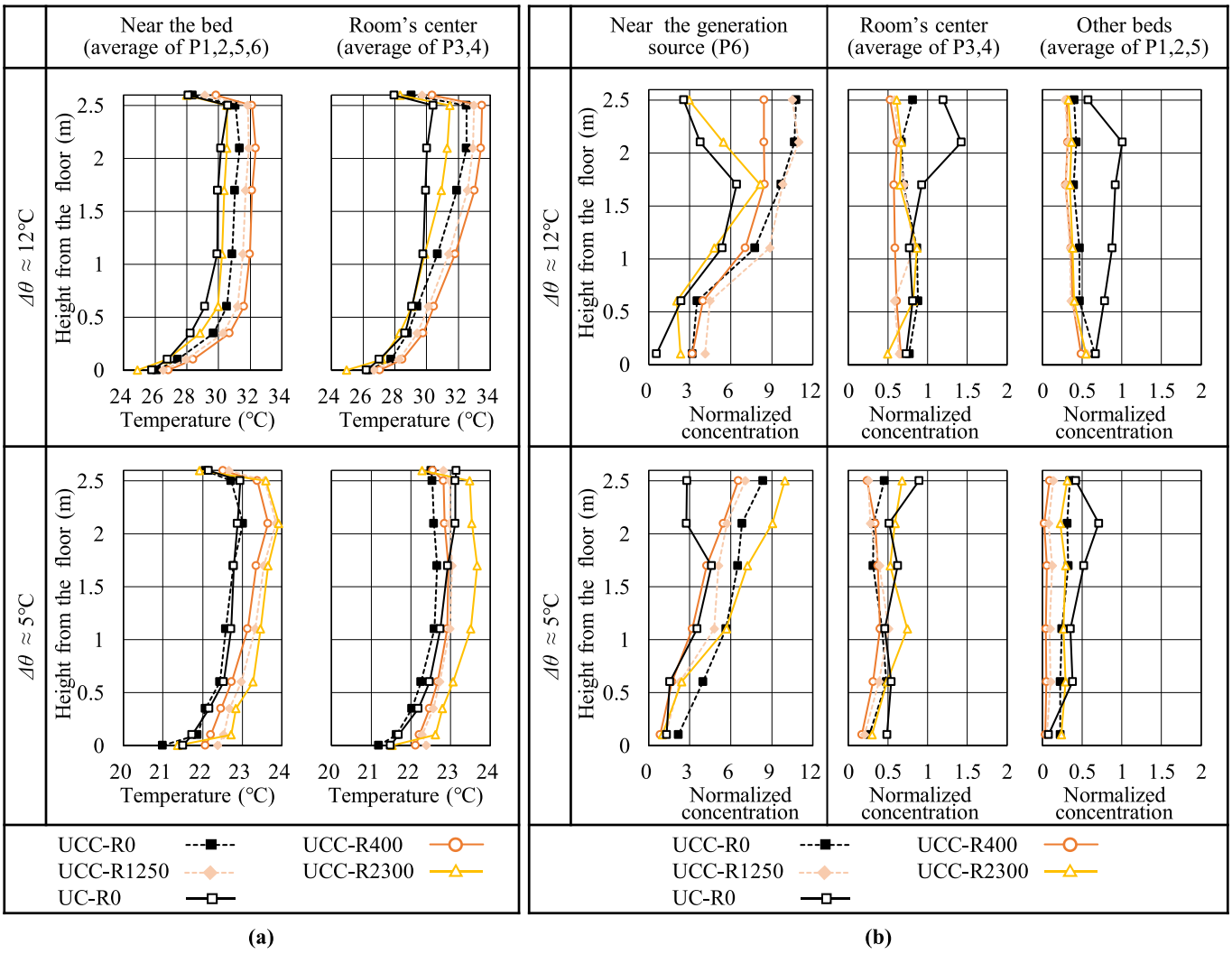


**Fig. 11.** Experimental results of heating and ventilation performance comparison when using the suspended cubicle curtain, ceiling-mounted cubicle curtain, ceiling-mounted cubicle curtain combination with perimeter roll curtain in different length. (a) Temperature vertical distribution. (b) Normalized concentration vertical distribution.

the room's occupied zone being around 0.5. This value can be improved to less than 0.5 when combined with a perimeter roll curtain.

Higher normalized concentrations were observed near the generation source with ceiling-mounted curtains compared to suspended mounted. Contaminants leaking from the bottom of the cubicle curtain into the central part of the room were confirmed by higher normalized concentration at 0.1m height from the floor.

In conclusion, using wall IUs with suspended cubicle curtains can reduce the normalized concentration around the bed by approximately 20 % compared to complete mixing ventilation (normalized concentration = 1). Installing partitions (roll curtains) near the windows or switching to ceiling-mounted cubicle curtains can further reduce the concentration by an additional 40 % by limiting the horizontal diffusion of contaminants that accumulate near the ceiling. This arrangement allows the heating supply air from the window-side IU to remain clean after mixing with the downdraft near the window, then cool down to diffuse into the occupied zone along the floor, resulting in an airflow pattern similar to displacement ventilation (DV) but achieved indirectly through the downdraft.

### 4.2. CFD numerical study

#### 4.2.1. Validation by comparison with experimental results

The numerically simulated temperature and normalized concentration distribution are compared with experimental data in Fig. 12. Four sets of results were selected, involving the use of a ceiling-mounted cubicle curtain, with or without a 2300 mm roll curtain, and temperature differences ($\Delta\theta$) of 5 °C and 12 °C. These cases ensure that the influence of both the roll curtain and the ceiling-mounted curtain is considered.

CFD results show similar temperature distributions to the experimental data, with errors mostly less than 0.5 °C near the beds and less than 1 °C at the room's center. Errors may arise from the radiation ratio of solid surfaces set at 0.9, inaccuracies in ASHRAE-based heat transfer coefficients [59], insufficient surface resolution for the specified floor and ceiling temperatures, and unmeasured heat from the measurement devices. Despite these issues, the temperature gradient and distribution are accurately simulated, and the minor temperature errors do not significantly affect concentration distribution results.

Regarding normalized concentration, its distribution characteristics, such as the gradient near the generation source and diffusion along the floor or in the room center, are reproduced in detail. Most values are predicted accurately, with errors mainly at points with large normalized

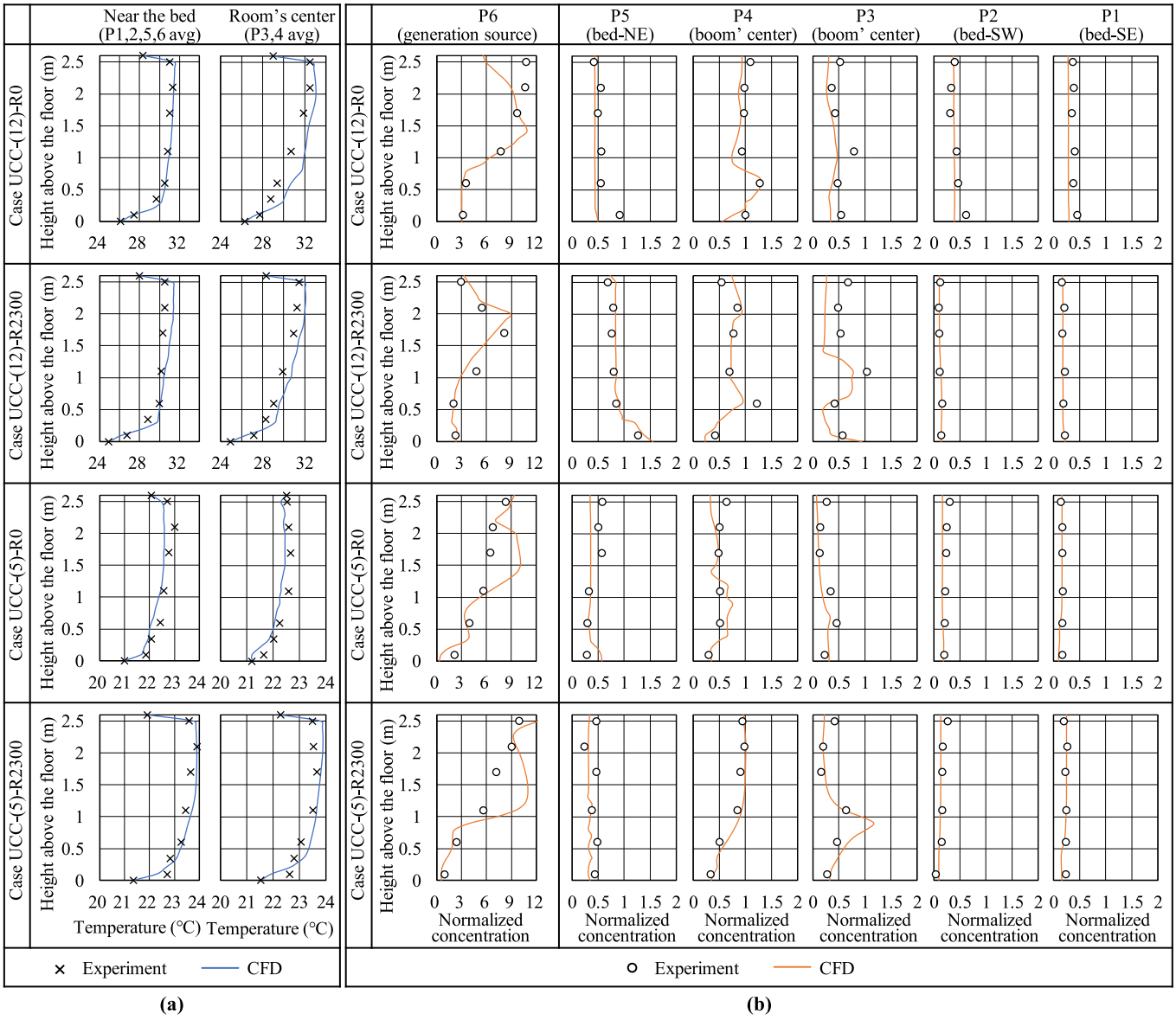


**Fig. 12.** Comparison of experimental data with CFD simulation results using the SKE model for validation. (a) Temperature distribution; (b) Normalized concentration distribution. Cases involve using the ceiling-mount cubicle curtain, with or without a 2300 mm roll curtain, and temperature difference (Δθ) is 5 °C or 12 °C.

concentration values. This discrepancy is due to the higher resolution of CFD data compared to experimental measurements and the amplification of normalized calculation errors at higher concentration values. Considering the study focuses on occupied space away from the generation source, their influence is negligible.

*4.2.2. Influence of curtains and airflow patterns*

Fig. 13 through Fig. 15 present the CFD results under harsher winter conditions compared to the experiment. The heat loss from the window is specified as 125 W/m$^2$, which roughly corresponds to an indoor and outdoor temperature difference of 20 °C and 35 °C when using double and single quartz glass windows, respectively.

Case using the wall IU and suspended cubicle curtain (UC-R0) is defined as the basic condition. The IU's PA temperature is fixed at 26 °C, ensuring an indoor temperature of around 24 °C under the ideal middle unit condition.

In addition to parameters such as the usage of the perimeter roll curtain and the comparison between suspended and ceiling-mounted cubicle curtains, further numerical comparisons were conducted by changing the ceiling center exhaust to four local exhausts (UC-R0-LoEx, Fig. 5(e)) and using the ceiling-mounted IU in the same ward (UC-R0-CeiIU, Fig. 5(f)).

Figs. 13 and ***14*** show the temperature and normalized concentration distribution in the ward, represented by line graphs for vertical distribution and contour graphs for representative sections of the entire room.

Regarding temperature distribution, the presence of the perimeter roll curtain can increase the vertical gradient to a certain extent when the cubicle curtain is suspended, especially near the floor, as observed by comparing the results of UC-R0 and UC-R800. However, this effect is limited when the cubicle curtain is ceiling mounted. Additionally, the ceiling-mounted cubicle curtain creates a more tortuous gradient around the near-bed space away from the window (Areas 2 and 4) compared to other scenarios. Moreover, the ceiling-mounted IU (UC-R0-CeiIU) increases the gradient in the room center, while the local exhaust (UC-R0-LoEx) has limited influence.

Overall, the curtain and airflow pattern do not significantly impact the temperature distribution in this study. They exhibit similar temperature distributions, with an approximate 1.5 °C vertical temperature

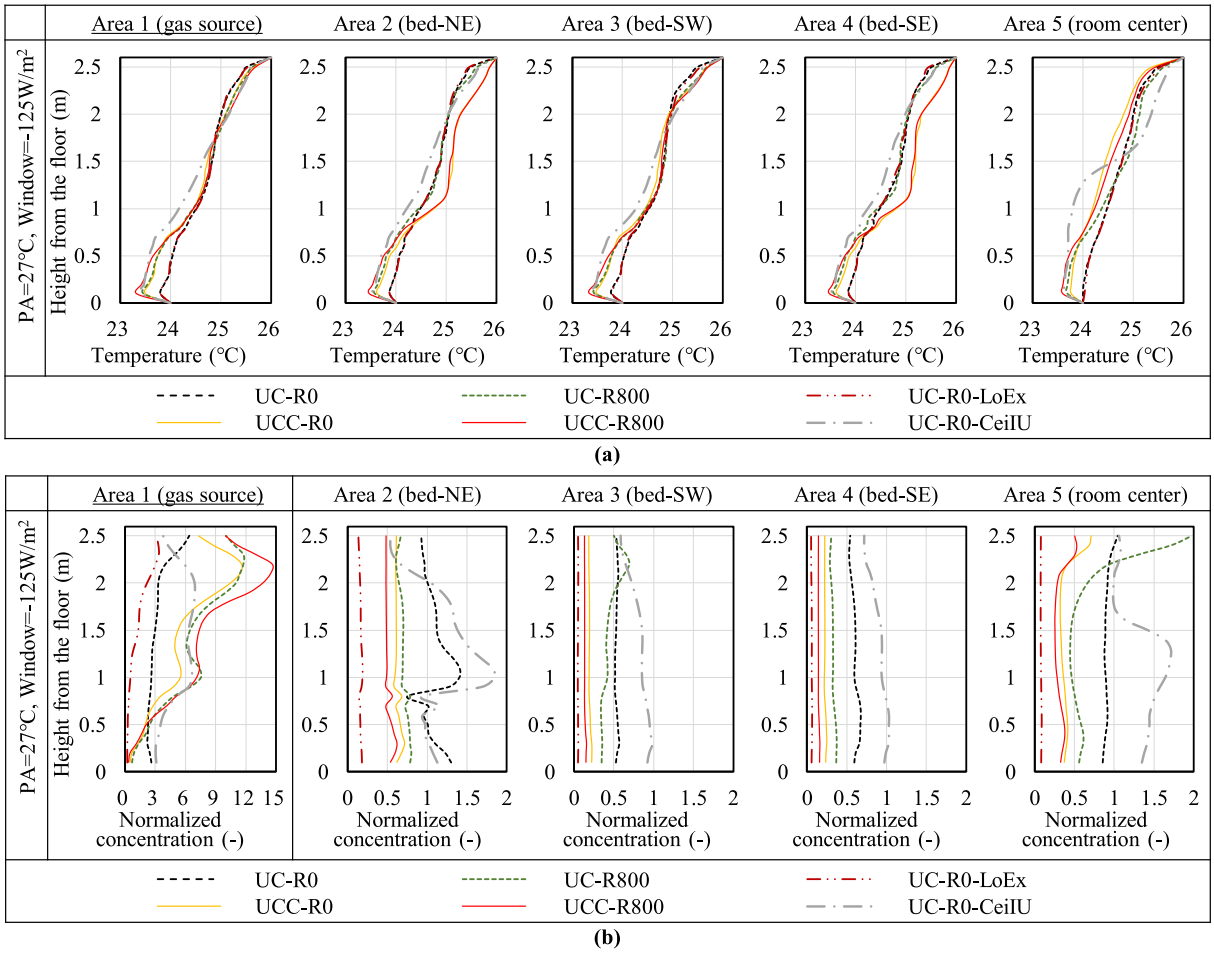


**Fig. 13.** Performance comparison of using suspended curtains, ceiling curtains, perimeter roll curtains, local exhaust, and ceiling IU (for mixing ventilation) under ideal conditions (window heat loss = 125 W/m$^2$, ceiling at 26 °C, floor at 24 °C, 27 °C supply air) based on CFD numerical results. (a) Temperature vertical distribution; (b) normalized concentration vertical distribution.

gradient in the occupied zone, meeting the conditions for DV and posing less risk of thermal discomfort. Only the temperature near the window is significantly influenced by the roll or ceiling-mounted curtain, as shown in Fig. 14, especially in the upper part of this space. This suggests that airflow exchange between the near-window space and the room's interior, particularly in the upper section, is limited or blocked by the presence of the ceiling-mounted or roll curtain.

Regarding the distribution of normalized concentrations shows in both Figs. 13 and 14, the basic condition (UC-R0) has a value of around 1 in the room center and around the bed next to the generation, and 0.7 around the other beds. The concentration near the generation source is lower than in other cases except for the local exhaust. The tracer gas was entrained into the downdraft near the window, then diffused along the floor to the space near bed-NE and the room center, which is considered the reason.

After installing the perimeter roll curtain or changing the suspended cubicle curtain to a ceiling mount (UC-R800, UCC-R0, and UCC-R800), the tracer gas's transport from the generation source to the near-window space is mostly blocked, ensuring that the airflow from the window side can diffuse into the interior with a low concentration value. However, these adjustments increase the normalized concentration value inside the cubicle space near the generation, causing airflow with high concentration to leak from the bottom opening of the cubicle curtain.

Using a ceiling-mounted curtain (UCC) results in lower normalized concentration than a suspended curtain overall, with values around 0.3 near beds opposite the source and 0.5 near beds next to the source or in the room center. Combining the ceiling-mounted cubicle and roll curtain provides the best ventilation performance in cases using the ceiling center exhaust, as it further limits contaminant spread to the room center from the near-ceiling area, decreasing concentration and reducing entrainment into the downdraft (see section #2 in Fig. 14, UC-R800 and UCC-R800).

Using local exhaust achieves the best ventilation. Although some diffusion near the window occurs, this setup achieves the lowest normalized concentration throughout the ward. No leakage from the cubicle curtain's bottom open space is observed, and upper room concentrations decrease significantly. Conversely, changing the IU from wall-mounted to ceiling-mounted results in the worst performance. The ceiling supply flow disrupts contaminants rising with the human plume, leading to disordered diffusion. Contaminants accumulate in the mid-height of the room, resulting in a normalized concentration greater than 2.

The mean normalized concentration in the breathing area of beds away from the generation is compared in Fig. 15*(a)* and ***(b)***, by case and by area, respectively. The probability of infection for occupants after a five-day stay with an infected individual is summarized in Fig. 15*(c)*.

Compared to the ceiling-mounted IU (UC-R0-CeilU) results in mixing ventilation, the vertical wall-mounted IU (UC-R0) reduces the inhaled normalized concentration for occupants opposite the infected individual through quasi-displacement ventilation, lowering the infection probability from around 40 %–25 %. Implementing a roll curtain near the window, switching to ceiling-mounted cubicle curtains, or combining

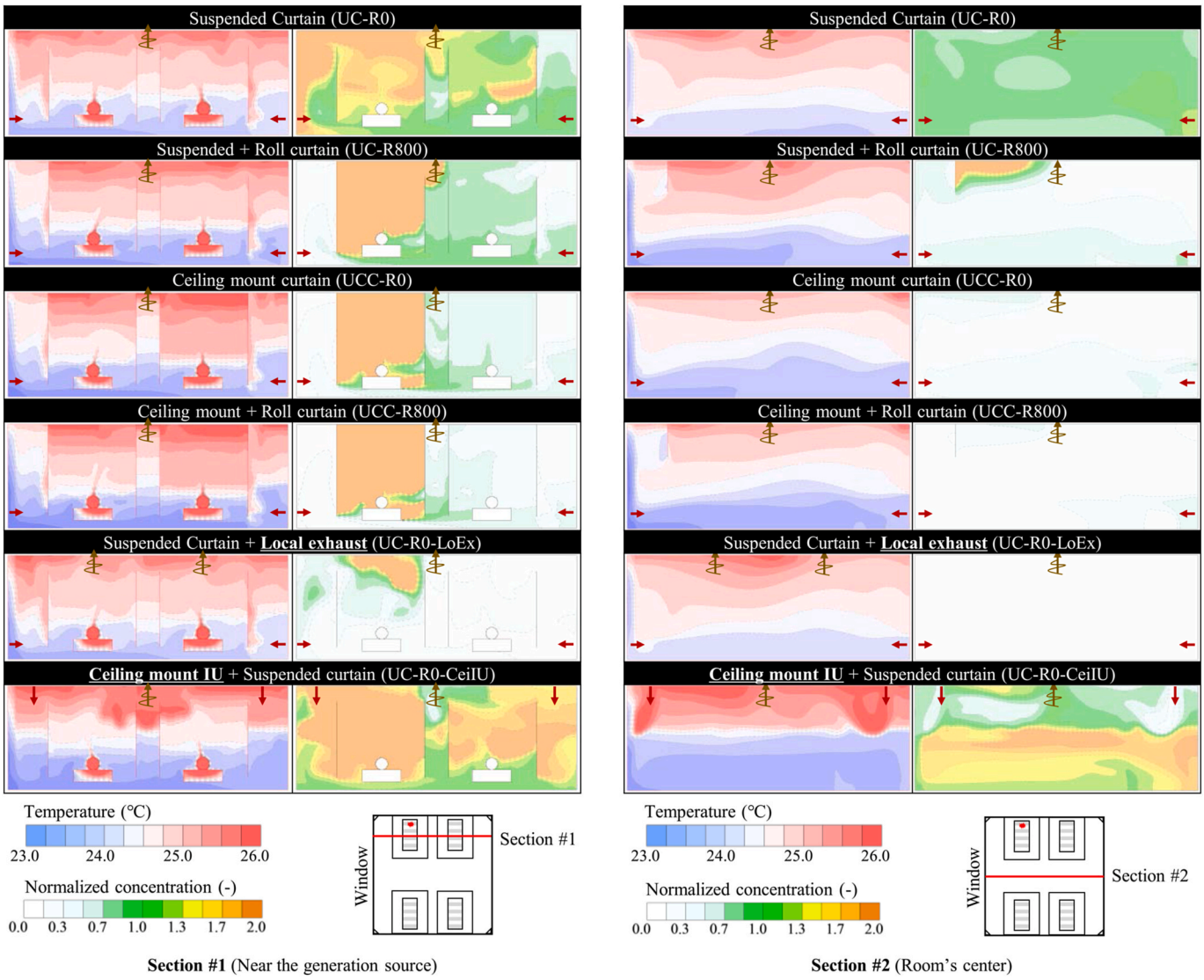


**Fig. 14.** Temperature and normalized concentration distribution in the ward when using suspended curtains, ceiling curtains, perimeter roll curtains, local exhaust, and ceiling IU (for mixing ventilation) under ideal conditions (window heat loss = 125 W/m$^2$, ceiling at 26 °C, floor at 24 °C, 27 °C supply air) based on CFD numerical results. (a) section distribution near the generation source; (b) section distribution in the room center.

both methods, further decreases concentration values and infection probability. This approach keeps the near-window area clean and indirectly achieves displacement ventilation, resulting in a normalized concentration of around 0.5 and a 24 % infection probability for the bed next to the infected individual, and less than 0.3 and 8 % for the bed opposite.

Furthermore, utilizing local exhaust is highly recommended, as it can further halve the inhaled concentration and infection probability compared to cases using the ceiling center exhaust.

#### 4.2.3. *Influence of the window heat loss*

The UCC-R800 (Fig. 5(d)), a four-bed ward with a vertical wall-mounted IU, a ceiling center exhaust, ceiling-mounted cubicle curtains, and an 800 mm perimeter roll curtain was chosen as the basic configuration. This setup is preferred for its ventilation improvement effects while still using the common ceiling center exhaust. The heat loss from the exterior window was adjusted from 0 to 150 W/m$^2$ to evaluate its influence. Fig. 16*(a)* shows the corresponding indoor and outdoor temperature differences for single or double quartz glass and double low-e glass windows under these various heat loss conditions.

Fig. 16(b)~(e) summarizes the room's vertical temperature distribution, normalized concentration distribution, and the mean normalized concentration in the breathing space of beds away from the generation source, respectively. Fig. 17 shows airflow exchanges from near the window to the room's interior, inside and outside the ceiling-mounted cubicle curtain, and the normalized concentration in representative sections for comparison.

Based on Fig. 16*(b)*, increased window heat loss generates a stronger cold draft, raising the vertical temperature gradient from 1 °C to 2 °C in the room center and from 1.5 °C to 2.5 °C near the bed. Cold draft from the window tends to flow towards the bed, likely due to heat sources such as occupants and equipment around the bed, which create heat plumes that draw in the cold window airflow.

In Fig. 16(c), (d), and 16(e), when window heat loss is 0, Areas 2 and 5 have the lowest normalized concentration values due to the absence of downdraft. With heat loss of 25 W/m$^2$, Areas 2 and 5 show significant concentration increases. This is considered that the heat loss generates a weak downdraft that is insufficient to adequately dilute or displace contaminants near the floor but complicates the flow field near the generation source. When the heat loss is 50–100 W/m$^2$, the concentration near bed-NE decreases, and showing a low value throughout the room. Furthermore, when the heat loss exceeds 100 W/m$^2$, the

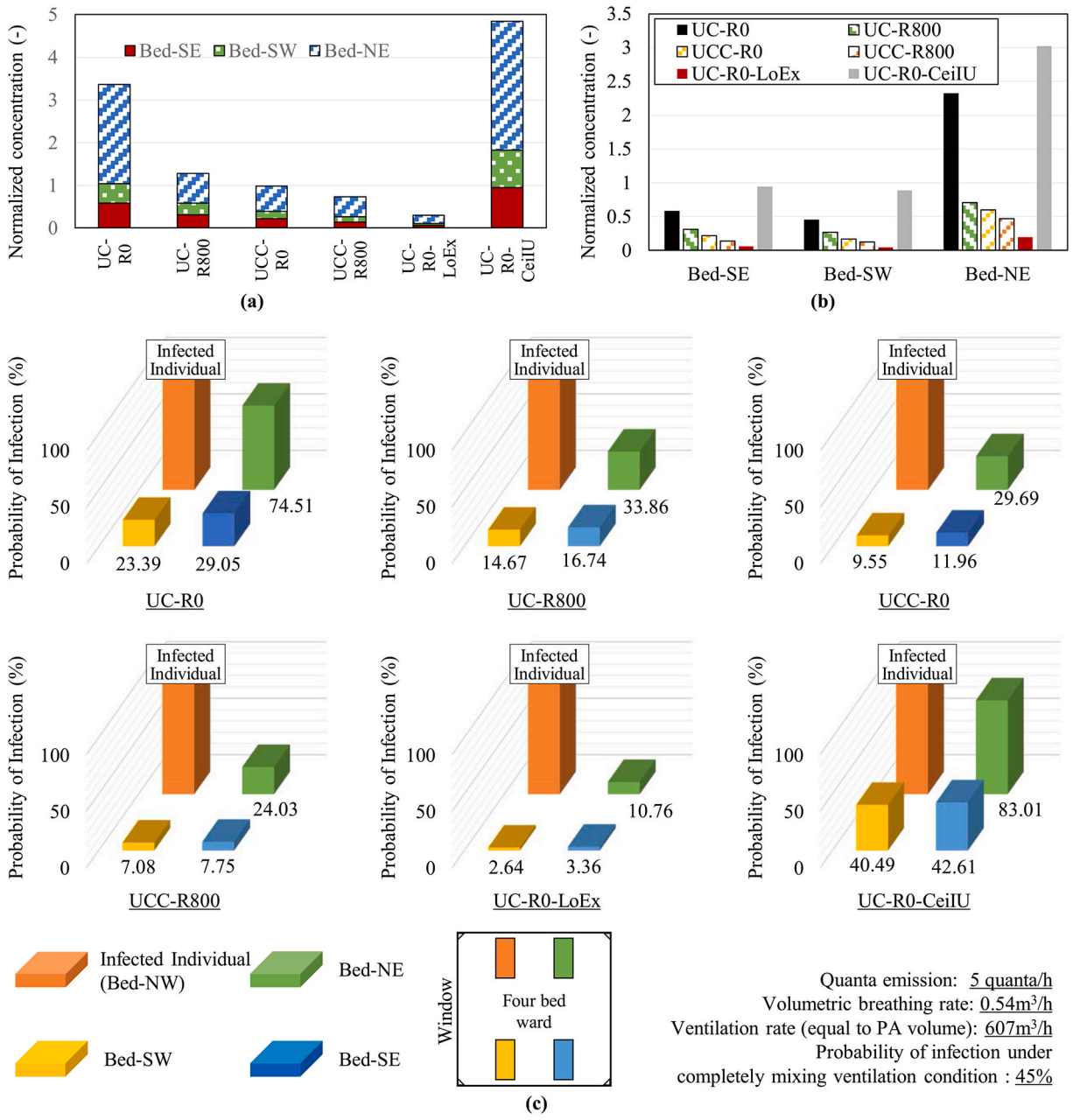


**Fig. 15.** Mean normalized concentration in the breathing area of beds away from the generation and the infection risk of the occupant lying in these beds for reference(a) mean normalized concentration compared by case; (b) mean normalized concentration compared by location; (c) five-day infection risk after staying with an infected individual.

normalized concentration value steadily increases with higher heat loss, that the value near bed NE becomes larger than 0.6 and around 0.3 generally.

Fig. 17 shows the airflow and concentration distribution results to support the above considerations. In Fig. 17*(a)*, the airflow to the room interior concentrates at the room's middle height (300–1800 mm from the floor) between the cubicle curtains when the window is isothermal. With heat loss of 25–75 W/m$^2$, the airflow shifts towards the perimeter, while the airflow along the floor directed towards the interior spreads across the entire room width with increasing velocity.

Fig. 17*(b)* shows the airflow rate through the roll curtain section, where negative values indicate airflow towards the perimeter and positive values indicate airflow towards the interior, aligning with the observations in Fig. 17*(a)*.

Fig. 17*(c)* shows the component velocity normal to the opening on the ceiling-mounted cubicle curtain facing the ceiling center exhaust, and the airflow rate passing through this opening. The flow rate does not initially increase proportionally to the heat load. It rises when the window shifts from isothermal to heat-losing, peaks around 25 W/m$^2$ of window heat loss, and then decreases with further heat loss. This is likely due to weaker downdrafts initially. As downdrafts strengthen with increased heat loss, the airflow entering the cubicle gains higher horizontal velocity, affecting the occupant's plume by decreasing the Archimedean number. However, the differences in exchange flow rate under different heat loss conditions are not very significant. This aspect warrants further investigation through detailed CFD analysis or developing a calculation model to predict airflow relationships and displacement ventilation surface layers under these conditions.

In conclusion, the isothermal window case exhibits the best ventilation performance due to the absence of downdraft. The optimal heat

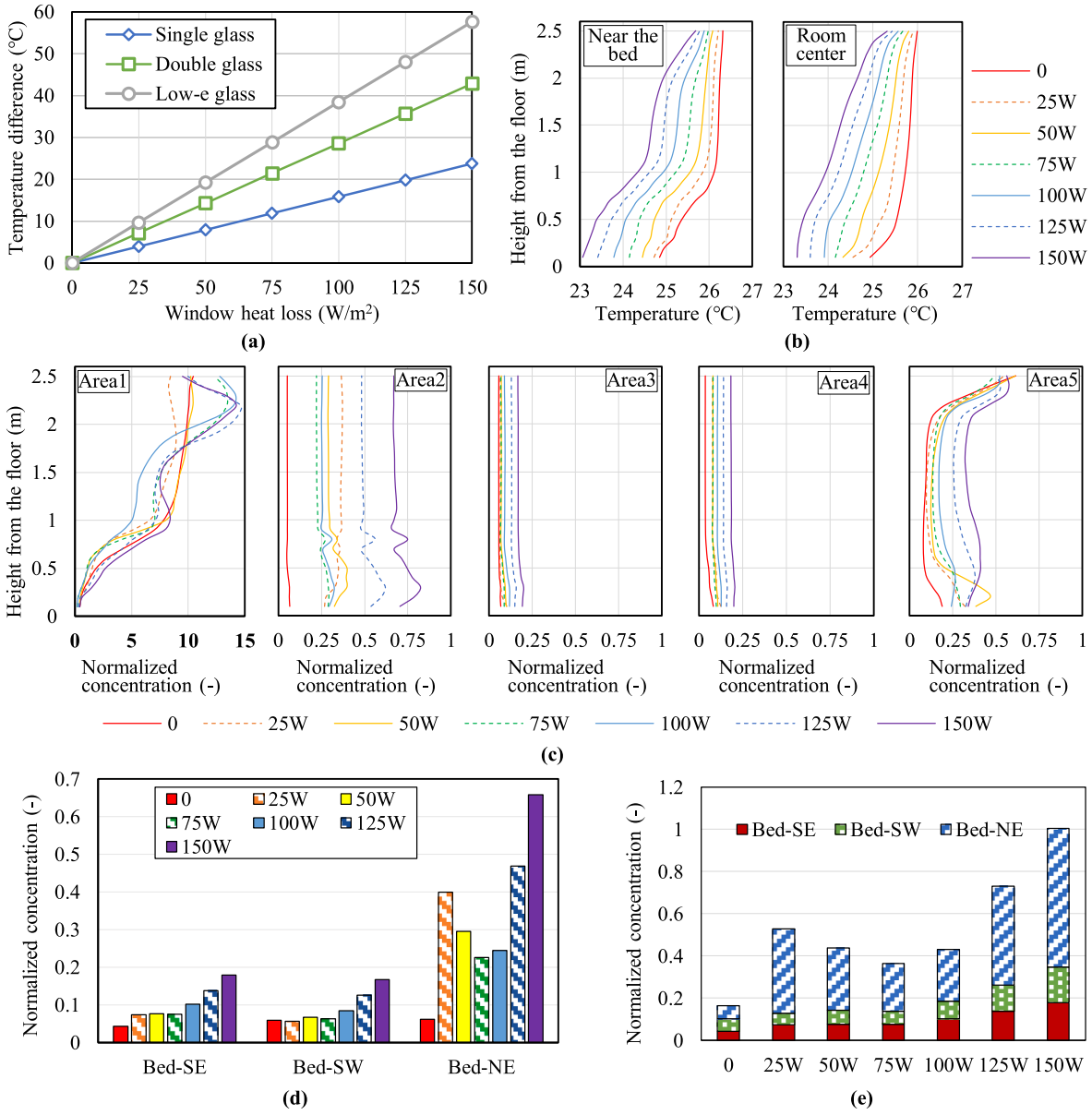


**Fig. 16.** Window heat loss's influence on the temperature and normalized concentration distribution (a) indoor and outdoor temperature difference corresponds to the window heat loss; (b) temperature vertical distribution; (c) normalized concentration vertical distribution; (d) mean normalized concentration in the breathing area compared by location; (e) mean normalized concentration in the breathing area compared by cases.

loss from the window to indirectly achieve displacement ventilation (DV) is approximately 75 W/m$^2$. This corresponds to indoor-outdoor temperature differences of 12 °C and 21 °C for single or double quartz glass, respectively, typical of temperate regions. Under this condition, the clean downdraft has a sufficient flow rate to displace and dilute contaminants near the floor while maintaining moderate velocity. However, when window heat loss exceeds 100 W/m$^2$, the indoor normalized concentration increases rapidly.

## 5. Conclusion

This study examines the ventilation efficiency of displacement ventilation (DV) systems under heating supply conditions through both experimental and numerical methods. Full-scale experiments were conducted to directly assess performance and provide comparison data for CFD validation. The CFD numerical study explored additional parameters under more controlled conditions, yielding comprehensive data for analysis. A four-bed ward equipped with a vertical wall-mounted induction air supply unit (IU) was selected for the case study.

The ventilation and thermal performance of the vertical wall-mounted IU in the ward during winter conditions were investigated, along with an analysis of why DV can still function to some extent during heating supply. In addition to buoyancy causing insufficient supply air to reach the occupied space, the presence of down drafts is identified as a significant factor in reducing DV efficiency. Implementing additional heating equipment near the window has proven effective in eliminating down drafts and maintaining DV stability. More importantly, limiting the horizontal movement of contaminants to keep the near-window space clean, and thereby indirectly achieving DV by utilizing the down drafts and the heating air supplied close to the window, is considered a simple and effective method to maintain good ventilation efficiency of the DV system during the heating season. The main conclusions drawn from this study are outlined below:

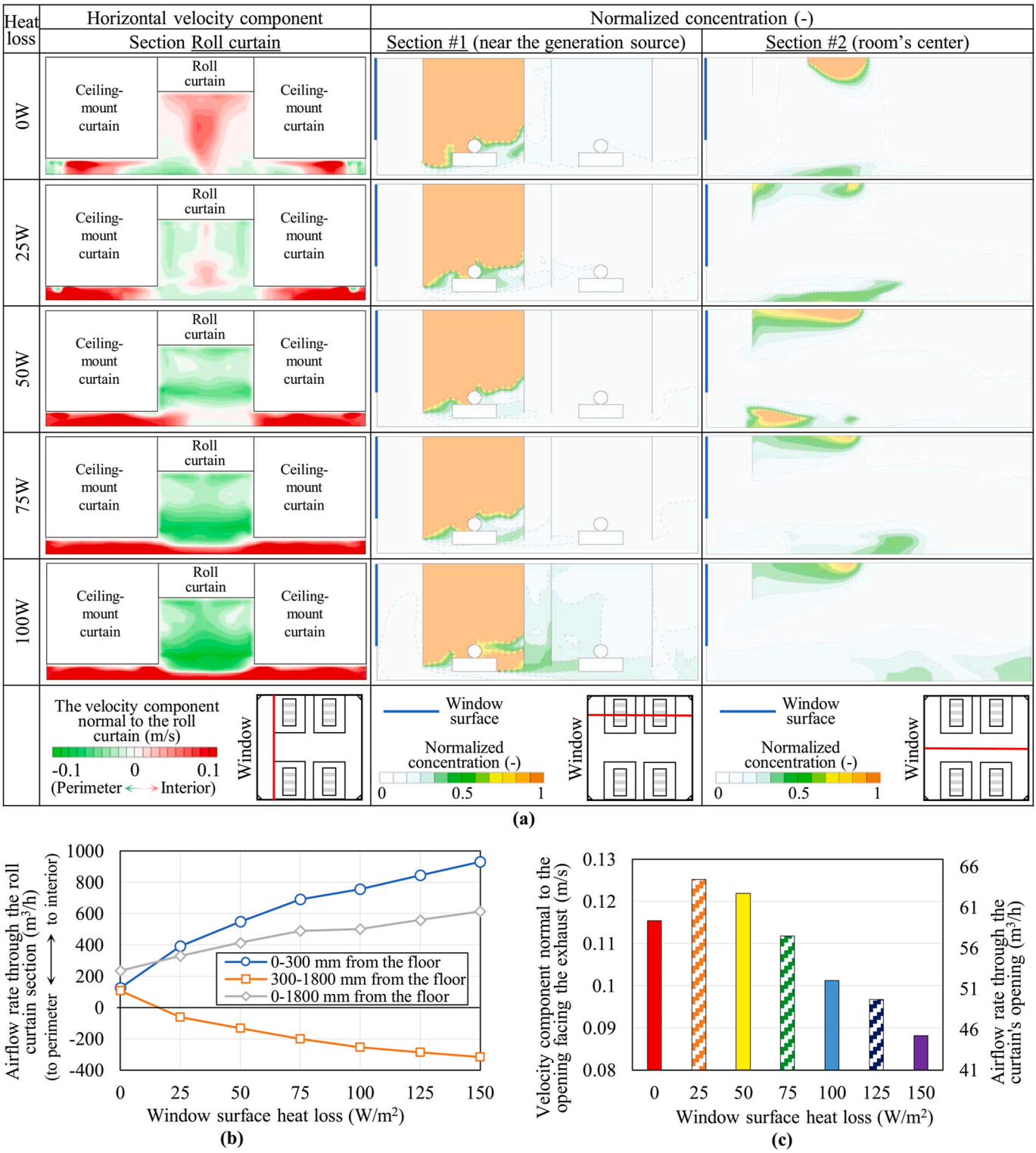


**Fig. 17.** Airflow exchange and concentration diffusion with window heat loss from 0 to 100 W (a) airflow exchange from near-window space to room interior and its impact on overall concentration distribution; (b) airflow rate through the opening below the cubicle curtain or room center near the window; (c) heat loss's impact on airflow exchange through the curtain's opening facing the exhaust.

- Quasi-displacement ventilation was achieved during the heating supply condition and in the presence of down draft. A vertical temperature gradient of around 3 °C was established in the ward, which is a prerequisite for conducting DV. However, some contaminants were entrained by the down draft and diffused back into the occupied space, resulting in a normalized concentration value of around 0.7 near other hospital beds away from the source. Nonetheless, this is still considered a better ventilation performance compared to the ideal mixing scenario, where the normalized concentration is 1.
- Down drafts away from the generation source, or with less mixing with contaminants, can remain clean or have a lower pollution rate. This clean airflow diffuses along the floor into the room, acting

similarly to supply air in a typical DV scenario. It supplements the insufficient clean airflow volume during heating and indirectly achieves DV.

- Without using the cubicle curtain around the generation source (the hospital bed in this study), contaminants risk being entrained into the down draft during the rising process, even directly after being generated. This results in a normalized concentration greater than 1 at the floor level, indicating that DV is mostly destroyed by uncontrolled airflow and contaminant diffusion.
- The suspended cubicle curtain cannot completely prevent contaminants from being entrained by the down draft, as they can diffuse through the gap between the curtain and ceiling. Switching to a ceiling-mounted curtain or adding a perimeter roll curtain can largely block the horizontal movement of contaminants toward the window, keeping the down draft clean and thereby improving indirect DV efficiency. Experimental results show a normalized concentration of 0.7 near the hospital bed with a suspended cubicle curtain, which decreases to around 0.5 with a perimeter roll curtain or ceiling-mounted curtain, and further improves to less than 0.5 when both measures are used.
- The length of the perimeter roll curtain has limited influence on indoor concentration and temperature distribution, according to experimental results. A too-short curtain risks contaminant crossover, while a too-long curtain inconveniences occupant. A length covering the height above the occupied space (higher than Fl+1800 mm) was chosen for numerical analysis, demonstrating good performance.
- The window curtain has little effect on indoor concentration and temperature distribution and cannot prevent contaminants from being entrained by the down draft. However, the window heater can eliminate down drafts by heating the window glass and generating a plume, thereby maintaining DV efficiency during winter and achieving a normalized concentration of around 0.3 away from the generation source.
- Scenarios using the ceiling-mounted IU for mixing ventilation and the combination of the vertical wall-mounted IU with local exhaust were also numerically compared with the abovementioned parameters. All cases using the wall-mounted IU showed better ventilation performance than the ceiling mounted. Using local exhaust achieved the best ventilation, even with only the suspended cubicle curtain and no perimeter roll curtain.
- The probability of infection for other occupants after a five-day stay with an infected individual was estimated using the Wells-Riley model. The probability is 40–83 % with the ceiling-mounted IU (depending on location), 23–75 % with the suspended cubicle curtain, 15–34 % with an added perimeter roll curtain, 10–30 % with the ceiling-mounted cubicle curtain, 7–24 % with both ceiling-mounted and perimeter curtains, and 3–11 % with the ceiling local exhaust and suspended cubicle curtain. And this value is 45 % when conducting the ideal mixing ventilation.
- The window heat loss value influences the ventilation performance of indirect DV. An isothermal window performs best due to the absence of downdraft. Insufficient heat loss (less than 25 $W/m^2$) impairs indirect DV by providing inadequate down draft to supply clean air along the floor and complicating airflow near the perimeter. Heat loss of 50–100 $W/m^2$ provides stable indirect DV, but over 100 $W/m^2$, normalized concentration significantly increases in the occupied space due to high-velocity floor-level airflow, which weakens contaminant rising and accelerates dispersion into the room interior.

In summary, this study introduces the mechanism of quasi-displacement ventilation under heating conditions. The proposed ventilation improvement method utilizes a curtain to block the horizontal movement of contaminants and down draft to supply clean air, thereby achieving indirect DV with higher ventilation performance, as demonstrated through experimental and numerical studies. The ventilation and thermal performance of the vertical wall-mounted induction unit (IU) for use in four-bed wards during the heating period were examined, echoing our series of works on the design methodology and cooling performance of this prototype air terminal device. Future research will focus on refining and quantifying indirect DV to further clarify and summarize its mechanism. Additionally, adjustments to the ceiling-mounted cubicle's opening area and investigations into air change rates inside and outside the cubicle area will be conducted to address excessive contaminant concentration near the source and mitigate leakage risks through the curtain's bottom opening.

## CRediT authorship contribution statement

**Shaoyu Sheng:** Writing – review & editing, Writing – original draft, Validation, Methodology, Investigation, Formal analysis, Data curation, Conceptualization. **Toshio Yamanaka:** Writing – review & editing, Supervision, Software, Resources, Project administration, Methodology, Funding acquisition, Conceptualization. **Tomohiro Kobayashi:** Writing – review & editing, Supervision, Software, Resources, Funding acquisition. **Nobukazu Chou:** Resources, Data curation.

## Declaration of competing interest

The authors declare that they have no known competing financial interests or personal relationships that could have appeared to influence the work reported in this paper.

## Data availability

Data will be made available on request.

## Acknowledgements

This work was supported by the KIMURA KOHKI Corporation.

## References

[1] A. Melikov, E. Mundt, P. Mustakallio, P.V. Nielsen, REHVA Guidebook No. 23: Displacement Ventilation, Kosonen, Risto, REHVA, 2017.
[2] Y. X, C. Q, G.L. R, A critical review of displacement ventilation [Online]. Available, https://www.aivc.org/resource/critical-review-displacement-ventilation, Jan. 1998. (Accessed 31 July 2023).
[3] O. Seppanen, W.J. Fisk, J. Eto, D.T. Grimsrud, Comparison of Conventional Mixing and Displacement Air Conditioning and Ventilating Systems in US Commercial Buildings, Lawrence Berkeley National Lab. (LBNL), Berkeley, CA (United States), Feb. 1989. LBL-26816; CONF-890609-2, https://www.osti.gov/biblio/6059781. (Accessed 6 June 2024).
[4] X. Zhao, Y. Yin, Hazards of pollutants and ventilation control strategy in industrial workshops: current state and future trend, Build. Environ. 251 (Mar. 2024) 111229, https://doi.org/10.1016/j.buildenv.2024.111229.
[5] H.-Q. Wang, et al., Fume transports in a high rise industrial welding hall with displacement ventilation system and individual ventilation units, Build. Environ. 52 (Jun. 2012) 119–128, https://doi.org/10.1016/j.buildenv.2011.11.004.
[6] Y. Lu, J. Huang, D.N. Wagner, Z. Lin, N. Jung, B.E. Boor, The influence of displacement ventilation on indoor carbon dioxide exposure and ventilation efficiency in a living laboratory open-plan office, Build. Environ. 256 (May 2024) 111468, https://doi.org/10.1016/j.buildenv.2024.111468.
[7] Z. Lin, T.T. Chow, C.F. Tsang, Effect of door opening on the performance of displacement ventilation in a typical office building, Build. Environ. 42 (3) (Mar. 2007) 1335–1347, https://doi.org/10.1016/j.buildenv.2005.11.005.
[8] Y. Wang, F.-Y. Zhao, J. Kuckelkorn, H. Spliethoff, E. Rank, School building energy performance and classroom air environment implemented with the heat recovery heat pump and displacement ventilation system, Appl. Energy 114 (Feb. 2014) 58–68, https://doi.org/10.1016/j.apenergy.2013.09.020.
[9] A. Essa, T. Yamanaka, T. Kobayashi, N. Choi, Effect of source location on contaminant dispersion pattern and occupants inhaled air quality in lecture room under displacement ventilation, Jpn. Archit. Rev. 6 (1) (2023) e12313, https://doi.org/10.1002/2475-8876.12313.
[10] T. Zhang, X. Liu, L. Zhang, J. Jiang, M. Zhou, Y. Jiang, Performance analysis of the air-conditioning system in xi'an xianyang international airport, Energy Build. 59 (Apr. 2013) 11–20, https://doi.org/10.1016/j.enbuild.2012.12.044.
[11] B. Zhuang, J. Shi, Z. Chen, Numerical study on indoor environment and thermal comfort in train station waiting hall with two different air-conditioning modes,

Build. Simulat. 14 (2) (Apr. 2021) 337–349, https://doi.org/10.1007/s12273-020-0732-0.
[12] T. Nishioka, K. Ohtaka, N. Hashimoto, H. Onojima, Measurement and evaluation of the indoor thermal environment in a large domed stadium, Energy Build. 32 (2) (Jul. 2000) 217–223, https://doi.org/10.1016/S0378-7788(00)00048-7.
[13] W. Lin, X. Liu, T. Zhang, Z. Zhou, Investigation of displacement and jet ventilation systems applied in an ice rink, J. Build. Eng. 50 (Jun. 2022) 104179, https://doi.org/10.1016/j.jobe.2022.104179.
[14] R. You, et al., An innovative personalized displacement ventilation system for airliner cabins, Build. Environ. 137 (Jun. 2018) 41–50, https://doi.org/10.1016/j.buildenv.2018.03.057.
[15] D. Schmeling, J. Bosbach, On the influence of sensible heat release on displacement ventilation in a train compartment, Build. Environ. 125 (Nov. 2017) 248–260, https://doi.org/10.1016/j.buildenv.2017.08.039.
[16] G. Zheng, C. Shen, A. Melikov, X. Li, Improved performance of displacement ventilation by a pipe-embedded window, Build. Environ. 147 (Jan. 2019) 1–10, https://doi.org/10.1016/j.buildenv.2018.10.006.
[17] A.K. Melikov, Advanced air distribution: improving health and comfort while reducing energy use, Indoor Air 26 (1) (2016) 112–124, https://doi.org/10.1111/ina.12206.
[18] F. Causone, F. Baldin, B.W. Olesen, S.P. Corgnati, Floor heating and cooling combined with displacement ventilation: possibilities and limitations, Energy Build. 42 (12) (Dec. 2010) 2338–2352, https://doi.org/10.1016/j.enbuild.2010.08.001.
[19] C. Gladstone, A.W. Woods, On buoyancy-driven natural ventilation of a room with a heated floor, J. Fluid Mech. 441 (Aug. 2001) 293–314, https://doi.org/10.1017/S0022112001004876.
[20] S. H, Floor heating and displacement ventilation [Online]. Available: https://www.aivc.org/resource/floor-heating-and-displacement-ventilation, Jan. 2003. (Accessed 16 June 2024).
[21] M. Krajčík, R. Tomasi, A. Simone, B.W. Olesen, Experimental study including subjective evaluations of mixing and displacement ventilation combined with radiant floor heating/cooling system, HVAC R Res. 19 (8) (Nov. 2013) 1063–1072, https://doi.org/10.1080/10789669.2013.806173.
[22] N. Choi, T. Yamanaka, K. Sagara, Y. Momoi, T. Suzuki, Displacement ventilation with radiant panel for hospital wards: measurement and prediction of the temperature and contaminant concentration profiles, Build. Environ. 160 (Aug. 2019) 106197, https://doi.org/10.1016/j.buildenv.2019.106197.
[23] S. Javed, I.R. Ørnes, T.H. Dokka, M. Myrup, S.B. Holøs, Evaluating the use of displacement ventilation for providing space heating in unoccupied periods using laboratory experiments, field tests and numerical simulations, Energies 14 (4) (Jan. 2021), https://doi.org/10.3390/en14040952. Art. no. 4.
[24] A.W. Woods, S. Fitzgerald, S. Livermore, A comparison of winter pre-heating requirements for natural displacement and natural mixing ventilation, Energy Build. 41 (12) (Dec. 2009) 1306–1312, https://doi.org/10.1016/j.enbuild.2009.07.030.
[25] B. Ouazia, A. Thompson, I. Macdonald, D. Booth, M. Tardif, Contaminant removal effectiveness of displacement ventilation systems during heating season; summary results from three field studies, ASHRAE Trans. 118 (2) (Oct. 2012) 292–299.
[26] A. Essa, et al., A novel portable cooling unit with air purification for displacement ventilation: parametric study with zonal model and field experiment, Build. Environ. 244 (Oct. 2023) 110657, https://doi.org/10.1016/j.buildenv.2023.110657.
[27] Y. Cho, H.B. Awbi, T. Karimipanah, Theoretical and experimental investigation of wall confluent jets ventilation and comparison with wall displacement ventilation, Build. Environ. 43 (6) (Jun. 2008) 1091–1100, https://doi.org/10.1016/j.buildenv.2007.02.006.
[28] H. Yin, A. Li, Z. Liu, Y. Sun, T. Chen, Experimental study on airflow characteristics of a square column attached ventilation mode, Build. Environ. 109 (Nov. 2016) 112–120, https://doi.org/10.1016/j.buildenv.2016.09.006.
[29] S. Sheng, T. Yamanaka, T. Kobayashi, Heating and ventilation performance investigation of a novel linear slot diffuser with adaptive outlet area for near window applications, Build. Environ. 244 (Oct. 2023) 110813, https://doi.org/10.1016/j.buildenv.2023.110813.
[30] H. Yin, et al., Numerical investigation on mechanisms and performance of column attachment ventilation for winter heating, Build. Environ. 202 (Sep. 2021) 108025, https://doi.org/10.1016/j.buildenv.2021.108025.
[31] H. Yamasawa, T. Kobayashi, T. Yamanaka, N. Choi, M. Cehlin, A. Ameen, Applicability of displacement ventilation and impinging jet ventilation system to heating operation, Jpn. Archit. Rev. 4 (2) (2021) 403–416, https://doi.org/10.1002/2475-8876.12220.
[32] T. Karimipanah, H.B. Awbi, Theoretical and experimental investigation of impinging jet ventilation and comparison with wall displacement ventilation, Build. Environ. 37 (12) (Dec. 2002) 1329–1342, https://doi.org/10.1016/S0360-1323(01)00117-2.
[33] J. Yoshihara, T. Yamanaka, T. Kobayashi, N. Choi, N. Kobayashi, Performance of combination of local exhaust system and floor-supply displacement ventilation system as prevention measure of infection in consulting room, Jpn. Archit. Rev. 6 (1) (2023) e12413, https://doi.org/10.1002/2475-8876.12413.
[34] F.S. Bauman, Designing and specifying underfloor systems: shedding light on common myths, Des. Specif. Underfloor Syst. Shedding Light Common Myths 75 (12) (2003) 26–39.
[35] M. Varia, et al., Investigation of a nosocomial outbreak of severe acute respiratory syndrome (SARS) in Toronto, Canada, CMAJ (Can. Med. Assoc. J.) 169 (4) (Aug. 2003) 285–292.
[36] D.E. Dimcheff, et al., Seroprevalence of severe acute respiratory syndrome coronavirus-2 (SARS-CoV-2) infection among Veterans Affairs healthcare system employees suggests higher risk of infection when exposed to SARS-CoV-2 outside the work environment, Infect. Control Hosp. Epidemiol. 42 (4) (Apr. 2021) 392–398, https://doi.org/10.1017/ice.2020.1220.
[37] M. Horiguchi, E. Shudo, K. Sato, M. Nakamura, W. Sai, T. Ohinata, Nurse odor perception in various Japanese hospital settings, Int. J. Nurs. Sci. 2 (4) (Dec. 2015) 355–360, https://doi.org/10.1016/j.ijnss.2015.08.009.
[38] M. Di Tella, A. Romeo, A. Benfante, L. Castelli, Mental health of healthcare workers during the COVID-19 pandemic in Italy, J. Eval. Clin. Pract. 26 (6) (2020) 1583–1587, https://doi.org/10.1111/jep.13444.
[39] H. Qian, Y. Li, P.V. Nielsen, C.E. Hyldgaard, T.W. Wong, A.T.Y. Chwang, Dispersion of exhaled droplet nuclei in a two-bed hospital ward with three different ventilation systems, Indoor Air 16 (2) (Apr. 2006) 111–128, https://doi.org/10.1111/j.1600-0668.2005.00407.x.
[40] H. Qian, Y. Li, P.V. Nielsen, C.E. Hyldgaard, Dispersion of exhalation pollutants in a two-bed hospital ward with a downward ventilation system, Build. Environ. 43 (3) (Mar. 2008) 344–354, https://doi.org/10.1016/j.buildenv.2006.03.025.
[41] Y. Yin, et al., Experimental study on displacement and mixing ventilation systems for a patient ward, HVAC R Res. 15 (6) (Nov. 2009) 1175–1191, https://doi.org/10.1080/10789669.2009.10390885.
[42] Y. Li, P. Nielsen, M. Sandberg, Displacement ventilation in hospital environments, ASHRAE J. 53 (6) (2011) 86–88.
[43] Displacement ventilation provides cornerstone of hospital design [Online]. Available, https://www.ashrae.org/technical-resources/ashrae-journal/featured-articles/displacement-ventilation-provides-cornerstone-of-hospital-design. (Accessed 17 June 2024).
[44] M. Chen, Y. Zhang, T. Li, Airborne spread of human coughing droplets with different postures and relative orientation in wards combined with peacetime and epidemic periods, Build. Environ. 245 (Nov. 2023) 110863, https://doi.org/10.1016/j.buildenv.2023.110863.
[45] S. Sheng, T. Yamanaka, T. Kobayashi, N. Choi, N. Chou, Performance of all-air wall induction unit for displacement ventilation in a four-bed hospital ward during the cooling period, Build. Environ. 248 (Jan. 2024) 111101, https://doi.org/10.1016/j.buildenv.2023.111101.
[46] Indoor Air Quality Handbook, McGraw-Hill, New York, 2001 [Online]. Available, http://archive.org/details/isbn_9780074455494. (Accessed 17 June 2024).
[47] M. Kanaan, N. Ghaddar, K. Ghali, G. Araj, Upper room UVGI effectiveness with dispersed pathogens at different droplet sizes in spaces conditioned by chilled ceiling and mixed displacement ventilation system, Build. Environ. 87 (May 2015) 117–128, https://doi.org/10.1016/j.buildenv.2015.01.029.
[48] H. Brohus, M. Hyldig, S. Kamper, U.M. Vachek, Influence of persons' movements on ventilation effectiveness: international conference on indoor air quality and climate, Proc. Indoor Air 2008 (2008).
[49] X. Cao, X. Dai, J. Liu, Building energy-consumption status worldwide and the state-of-the-art technologies for zero-energy buildings during the past decade, Energy Build. 128 (Sep. 2016) 198–213, https://doi.org/10.1016/j.enbuild.2016.06.089.
[50] A.S. Azad, et al., Evaluation of thermal comfort criteria of an active chilled beam system in tropical climate: a comparative study, Build. Environ. 145 (Nov. 2018) 196–212, https://doi.org/10.1016/j.buildenv.2018.09.025.
[51] R. Ming, et al., Effect of active chilled beam layouts on ventilation performance and thermal comfort under variable heat gain conditions, Build. Environ. 228 (Jan. 2023) 109872, https://doi.org/10.1016/j.buildenv.2022.109872.
[52] Y. Li, T. Yamanaka, H. Kotani, K. Sagara, Y. Momoi, M. Kuranaga, Effects of ceiling induction diffusers on indoor environmental quality of sickroom under the cooling air supply condition, Int. J. Vent. 17 (4) (Oct. 2018) 287–302, https://doi.org/10.1080/14733315.2018.1431360.
[53] L.I. Ying, Y. Toshio, K. Hisashi, S. Kazunobu, M. Yoshihisa, K. Mari, Experimental study on indoor environmental quality for four-bed ward with ceiling induction diffusers under heating condition, Trans. Soc. Heat. Air-Cond. Sanit. Eng. Jpn. (256) (2018) 19–28.
[54] S. Sheng, T. Yamanaka, T. Kobayashi, N. Choi, N. Chou, Experimental study and CFD modelling of four-bed hospital ward with all-air wall induction unit for air-conditioning, Build. Environ. 222 (Aug. 2022) 109388, https://doi.org/10.1016/j.buildenv.2022.109388.
[55] D.T. Pritchard, J.A. Currie, Diffusion of coefficients of carbon dioxide, nitrous oxide, ethylene and ethane in air and their measurement, J. Soil Sci. 33 (2) (1982) 175–184, https://doi.org/10.1111/j.1365-2389.1982.tb01757.x.
[56] REHVA COVID-19 guidance V4.1 [Online]. Available: https://www.rehva.eu/activities/covid-19-guidance/rehva-covid-19-guidance, 2021.
[57] S. Galmiche, et al., SARS-CoV-2 incubation period across variants of concern, individual factors, and circumstances of infection in France: a case series analysis from the ComCor study, Lancet Microbe 4 (6) (Jun. 2023) e409–e417, https://doi.org/10.1016/S2666-5247(23)00005-8.
[58] Y. Wu, L. Kang, Z. Guo, J. Liu, M. Liu, W. Liang, Incubation Period of COVID-19 caused by unique SARS-CoV-2 strains: a systematic review and meta-analysis, JAMA Netw. Open 5 (8) (Aug. 2022) e2228008, https://doi.org/10.1001/jamanetworkopen.2022.28008.
[59] American Society of Heating, Refrigerating and Air-Conditioning Engineers, Inc., *ASHRAE Handbook: Fundamentals*, American Society of heating, refrigerating and air-conditioning engineers, 2013.